Original Article

OPEN

SPARC–Dependent Cardiomyopathy in *Drosophila*

Paul S. Hartley, PhD; Khatereh Motamedchaboki, PhD; Rolf Bodmer, PhD; Karen Ocorr, PhD

Background—The *Drosophila* heart is an important model for studying the genetics underpinning mammalian cardiac function. The system comprises contractile cardiomyocytes, adjacent to which are pairs of highly endocytic pericardial nephrocytes that modulate cardiac function by uncharacterized mechanisms. Identifying these mechanisms and the molecules involved is important because they may be relevant to human cardiac physiology.

Methods and Results—This work aimed to identify circulating cardiomodulatory factors of potential relevance to humans using the *Drosophila* nephrocyte–cardiomyocyte system. A Kruppel-like factor 15 (*dKlf15)* loss-of-function strategy was used to ablate nephrocytes and then heart function and the hemolymph proteome were analyzed. Ablation of nephrocytes led to a severe cardiomyopathy characterized by a lengthening of diastolic interval. Rendering adult nephrocytes dysfunctional by disrupting their endocytic function or temporally conditional knockdown of *dKlf15* led to a similar cardiomyopathy. Proteomics revealed that nephrocytes regulate the circulating levels of many secreted proteins, the most notable of which was the evolutionarily conserved matricellular protein Secreted Protein Acidic and Rich in Cysteine (SPARC), a protein involved in mammalian cardiac function. Finally, reducing *SPARC* gene dosage ameliorated the cardiomyopathy that developed in the absence of nephrocytes.

Conclusions—The data implicate SPARC in the noncell autonomous control of cardiac function in *Drosophila* and suggest that modulation of *SPARC* gene expression may ameliorate cardiac dysfunction in humans. **(*Circ Cardiovasc Genet*. 2016;9:119-129. DOI: 10.1161/CIRCGENETICS.115.001254.)**

Key Words: animal models ■ cardiomyopathy ■ *Drosophila* ■ genetics ■ proteomics

Heart disease is a major cause of mortality worldwide, so identifying mechanisms that regulate cardiac physiology is a crucial step toward its treatment and prevention. Both vertebrate and invertebrate models contribute to our understanding of cardiovascular physiology and the related disease processes affecting humans. The *Drosophila* heart comprises contractile cardiomyocytes and neighboring pericardial nephrocytes that clear circulating colloids, macromolecules, and immune peptides from the hemolymph (blood).[1–3] This organ system has proven to be a tractable model that permits genetic screens to identify novel pathways relevant to human cardiac performance.[4] In addition, functional studies have contributed to our understanding of how alterations in structural proteins, including adhesion proteins such as fermitins/kindlins[5] and contractile proteins, such as myosin and troponin-T, translate to cardiomyopathy.[6] In addition, *Drosophila* has facilitated the elucidation of genetic pathways regulating cardiac aging[7,8] and diet-induced cardiac and kidney podocyte dysfunction.[9–11]

Editorial see p 104
Clinical Perspective on p 129

There is evidence that cardiac phenotypes develop in the *Drosophila* model as a result of nephrocyte dysfunction; however, the mechanisms are not well characterized.[12–15] It has also been reported that these cardiac phenotypes may depend on developmental changes to the nephrocyte–cardiomyocyte niche rather than a contribution by nephrocytes to cardiac homeostasis in adulthood.[16] Characterizing the noncell autonomous regulation of heart function in flies is important because it may provide insights into molecules that regulate human cardiac physiology.

The *Drosophila* ortholog of the mammalian transcription factor *Klf15* (also known as Kidney Kruppel-like factor) has recently been identified as a nephrocyte-restricted gene critical for the cells' differentiation and function.[17] Pericardial nephrocytes in flies homozygous for a *dKlf15* loss of function allele develop normally during embryonic cardiogenesis but then fail to differentiate during larval development and undergo attrition before pupation, hence adult flies have no pericardial

Received August 31, 2015; accepted January 27, 2016.

From the Department of Life and Environmental Science, University of Bournemouth, Dorset, United Kingdom (P.S.H.); and Proteomics Facility (K.M.) and Development, Aging, and Regeneration Program (R.B., K.O.), Sanford Burnham Prebys Medical Discovery Institute, La Jolla, CA.

The Data Supplement is available at http://circgenetics.ahajournals.org/lookup/suppl/doi:10.1161/CIRCGENETICS.115.001254/-/DC1.

Correspondence to Paul S. Hartley, PhD, Department of Life and Environmental Science, University of Bournemouth, Talbot Campus, Poole, Dorset BH12 5BB, United Kingdom. E-mail phartley@bournemouth.ac.uk or Karen Ocorr, PhD, Sanford Burnham Prebys Medical, Discovery Institute, 10901 N Torrey Pines Rd, La Jolla, CA 92037. E-mail kocorr@sbpdiscovery.org

nephrocytes. This enables the nephrocytes' impact on the circulating proteome in adults to be analyzed and for nephrocyte-dependent cardiomyocyte control mechanisms to be identified.

In this work, we took advantage of the nephrocyte–cardiomyocyte system in *Drosophila* to identify circulating cardiomodulatory factors of potential relevance to humans. Proteomics was used to establish the composition of the circulating proteome in flies with and without nephrocytes. It was found that either the loss of nephrocytes or their function during development led to cardiomyopathy, and contrary to previous reports, loss of nephrocyte function in adulthood also led to cardiomyopathy. Analysis of the hemolymph proteome established that nephrocytes had a broad impact on the circulating secretome. By coupling the proteomics data with genetic experiments, we showed that nephrocytes regulated circulating levels of the matricellular protein secreted protein acidic and rich in cysteine (SPARC) and prevent SPARC-dependent cardiomyopathy. SPARC plays multiple roles in mammals. SPARC levels increase in metabolic syndrome and aging, and it is well documented as contributing to pathological tissue fibrosis; however, reduced *SPARC* expression can lead to heart rupture in pressure overload models.[18] The current findings suggest that SPARC's role in the mammalian heart may be evolutionarily conserved and that its modulation may ameliorate cardiac dysfunction. The work also highlights the importance of *Drosophila* for the identification and study of cardiomodulatory signals of relevance to human cardiac physiology.

Materials and Methods

Strains Used in This Study

The w^{1118} (used as wild-type strain in this study), $dKlf15^{NN}$ (*CG2932*, FBgn0025679; previously known as $Bteb2^{f06447}$ was described in the study by Ivy et al[17]), *Dorothy-Gal4* (*dot-Gal4*, originally described in the study by Kimbrell et al[19]), *UAS-mCherry* (TRiP control line), $dSparc^{MI00329}$ (with an MiMIC insertion in the 5-prime region of the *dSparc* locus; as described in the study by Venken et al[20]), and $Tub\text{-}Gal80^{ts}$ lines were all from the Bloomington Stock Center (Bloomington, IL). The *HandC-Gal4* (*Hand-Gal4*) line was described in the study by Sellin et al[21]). The 2 RNAi lines for knocking-down *dKlf15* were from the Vienna Drosophila RNAi stock Center (with a targeting hairpin inserted into the second chromosome, VDRC) and Bloomington ($Klf15^{JF02420}$, a Harvard TRiP line with a *dKlf15* targeting hairpin inserted into the third chromosome). All genetic combinations were generated by standard crosses. Generation of TARGET flies (*Hand-Gal4*; $Tub\text{-}Gal80^{ts}$) was achieved by standard crosses.[22]

Husbandry and Propagation of Flies

Flies were propagated routinely on a cornmeal-molasses diet at 25°C under a 12:12 hour light:dark schedule. For TARGET experiments, flies were reared at 18°C and then transferred to 29°C within 1 to 5 days of eclosing. Flies remained at 29°C for 1 to 2 weeks. After analysis of heart function, flies were transferred to 25°C for 24 hours. To reduce the effect of genetic background, the $dKlf15^{NN}$ mutant was backcrossed onto the w^{1118} for >20 generations.

Quantitative PCR

See Methods section in the Data Supplement.

Imaging the Adult Heart

See Methods section for more detailed description of the method in the Data Supplement. Unless stated otherwise, 2- to 3-week-old adult female flies were anaesthetized with Flynap (Carolina Biological Supply Company, Burlington, NC), dissected and hearts stained as described previously.[5,23]

Analysis of Adult Heart Function

Two- to three-week-old adult flies were anesthetized with Flynap (Carolina Biological Supply Company), and the beating adult heart in semi-intact preparations was visualized with an Ionoptix Myocam S high frame rate video camera (Ionoptix Ltd, Dublin, Ireland) attached to a Zeiss AxioLab A1 with a water-dipping 10× objective. Approximately 15 s of video footage was collected using Micro-Manager open source microscopy software,[24] with a frame rate capture of between 120 and 150 frames per second. Videos were converted to audio video interleave files using ImageJ and analyzed using semiautomated optical heart analysis software,[25] www.sohasoftware.com; as previously described.[5] Quantified data are presented as the mean (±SEM) of at least 20 different flies per genotype.

Epifluorescence Microscopy of Adult Fly Tissues

See Methods section in the Data Supplement.

Collection of Hemolymph From Adult Flies

One-week-old adult female flies were rendered immobile at 4°C for 5 minutes. To remove contaminating food and feces flies were placed into a 1.5-mL centrifuge tube and 500-µL of 50% ice cold ethanol in water and the tube upturned several times. This step was repeated a further 2×, first with 50% ethanol and then with 50-mmol/L ammonium bicarbonate. Flies were then tipped onto an upturned 30-mm petri dish containing ice. The dorsal cuticle of the thorax of at least 100 flies was pricked with a 25G needle and then flies were collected into a centrifuge tube containing a 0.2-µm filter insert and 1 mL of 50-mmol/L ammonium bicarbonate. Flies were centrifuged at 4°C for 10 s at 2000 rpm (g value, 448g). The filtrate was removed and replaced into the upper filter cassette and centrifuged again. This step was repeated once more. The protein concentration of the filtrate was quantified by the Bradford assay using 50-mmol/L ammonium bicarbonate as a blank. Samples from flies that had not been pricked contained no protein. Samples contained 100 to 150 µg of total protein and were frozen at −20°C; volumes were adjusted with 50-mmol/L ammonium bicarbonate to normalize the total protein content between the samples. The mean spectral count of 3 independent biological replicates from the reference (w^{1118}) and $dKlf15^{NN}$ mutant genotypes was used to infer protein abundance.

Proteomic and Bioinformatics Analysis of Hemolymph Proteome

Hemolymph samples were lyophilized and resuspended in 200 µL with 50-mmol/L ammonium bicarbonate. Protein reduction was done by adding 4 µL of Tris(2-carboxyethyl)phosphine to 200 µL of samples at 60°C for 30 minutes. Iodoacetamide was added (to 20 mmol/L), and proteins were alkylated at 30 minutes at room temperature in the dark. Mass spectrometry grade trypsin (Promega) was added (1:20 ratio) for overnight digestion at 37°C on thermomixer set on 700 rpm. After digestion, formic acid was added to the peptide solution (to 2%), followed by desalting by Microtrap (Michrom-Bruker) and then on-line analysis of peptides by high-resolution, high-accuracy LC–MS/MS, consisting of a Michrom HPLC, an Agilent Zorbax C18 peptide trap, a 15-cm Michrom Magic C18 column, a low-flow ADVANCED Michrom MS source, and an LTQ-Orbitrap XL (Thermo Fisher Scientific). A 120-minute gradient of 10% to 30%B (0.1% formic acid and 100% acetonitrile) was used to separate the peptides. The total LC time was 140 minutes. The LTQ-Orbitrap XL was set to scan precursors in the Orbitrap followed by data-dependent MS/MS of the top 10 precursors. The LC–MS/MS raw data were submitted to Sorcerer Enterprise v.3.5 release (Sage-N Research Inc) with

SEQUEST algorithm as the search program for peptide/protein identification. SEQUEST was set up to search the target-decoy Swiss-Prot *Drosophila melanogaster* fasta protein database indexed with trypsin for enzyme with the allowance of ≤2 missed cleavages, Semi Tryptic search, and precursor mass tolerance of 50 ppm. The search results were viewed, sorted, filtered, and statically analyzed by using comprehensive proteomics data analysis software, Peptide/Protein prophet v.4.6.1 (Institute for Systems Biology, Seattle). The minimum transproteomic pipeline protein probability score was set to 0.8 to 0.90, to assure low error (much less than false discovery rate 2%) with reasonably good sensitivity. The differential spectral count analysis was done by QTools, an open source in-house developed tool for automated differential peptide/protein spectral count analysis and Gene Ontology.[26] SignalP 4.1 was used to identify proteins having a signal peptide sequence in their N terminus; default settings with a D cutoff of 0.45 were used.[27]

Statistics

When >2 genotypes or treatments were used in an experiment, 1-way ANOVA was used to test the hypothesis that genotype may have affected heart function, and post hoc test (Tukey honest significant difference) was used to establish *P* values between control and the different genotypes. An unpaired 2-tailed student's *t* test was used to compare 2 means. GeneProf[28] was used to calculate the probability that hemolymph samples may be enriched with proteins predicted to have an N-terminal signal peptide versus a background data set (the proportion of all known Drosophila genes predicted to encode for an N-terminal signal peptide).

Results

Genetic Ablation of Nephrocytes Using *dKlf15* Loss of Function

It has recently been demonstrated that *dKlf15* is a nephrocyte-restricted transcription factor critical for the viability and differentiation of *Drosophila's* 2 nephrocyte populations, the garland cells and pericardial nephrocytes.[17] In flies homozygous for a *dKlf15* loss of function allele (*dKlf15^{NN}*), the nephrocyte populations undergo attrition during late embryogenesis (garland cells, compare Figure 1B′ and 1B″ and the L3 stage of larval development, so that adults are completely devoid of nephrocytes (compare Figure 1A′ and 1A″).

Loss of Nephrocyte *dKlf15* Expression Leads to Cardiomyopathy

It is increasingly clear that *Drosophila* heart function is modulated by noncell autonomous mechanisms controlled by the neighboring pericardial nephrocytes.[14,15] To confirm that nephrocytes modulate cardiac function in the *Drosophila* model, adult hearts in wild-type and *dKlf15^{NN}* mutants were monitored by videomicroscopy. Homozygous *dKlf15^{NN}* mutant females (and hemizygous *dKlf15^{NN}* mutant males) had significantly longer heart periods (the time between the initiation of successive cardiac contractions) compared with controls, primarily because of a significant lengthening of the diastolic interval (Figure 2A and 2B for data from males see below). The mutants also had a modest increase in the arrhythmicity index (Figure 2B), a measure of the heart's beat-to-beat variability. In addition, end-diastolic and end-systolic diameters (EDD and ESD) were greater in mutants than in controls; however, this was not associated with a change in fractional shortening (the ratio of EDD to ESD—the relative distance that the heart wall travels during a contraction). To establish if the heart phenotype was because of the specific loss of nephrocyte *dKlf15* expression, *dKlf15* was silenced specifically in nephrocytes using *dorothy-Gal4*. Knockdown of *dKlf15* in nephrocytes led to a heart phenotype that was almost identical to that of the *dKlf15^{NN}* mutants; however, the arrhythmicity index, although trending toward being increased, was not statistically different from that of the controls (Figure 2B).

Nephrocytes Mediate Normal Cardiac Function in Adults

There is a doubt as to whether normal heart function in adult flies is dependent or not on sustained interactions between cardiomyocytes and nephrocytes. Sustained *dKlf15* expression is required for adult nephrocyte function,[17] so to establish if nephrocytes were required for normal cardiac function in adult flies, the TARGET system[22] was used to silence *dKlf15* in the nephrocytes of adult flies (Figure 3). Using this system, it was possible to allow functional nephrocytes to develop normally and then silence *dKlf15* in adults to cause nephrocyte dysfunction. Accordingly, nephrocytes dedifferentiated (showed reduced Amnionless protein expression) and lost their ability to accumulate dextran. In association with this, the flies developed a cardiomyopathy, which recapitulated that seen in the *dKlf15^{NN}* mutants as well as *dorothy-Gal4*–driven *dKlf15* silencing experiments (Figure 3B).

Reduction of Nephrocyte *Amnionless* Expression Is Associated With Cardiomyopathy

Amnionless is crucial for nephrocyte function,[29] so it was hypothesized that loss of *Amnionless* may be sufficient to

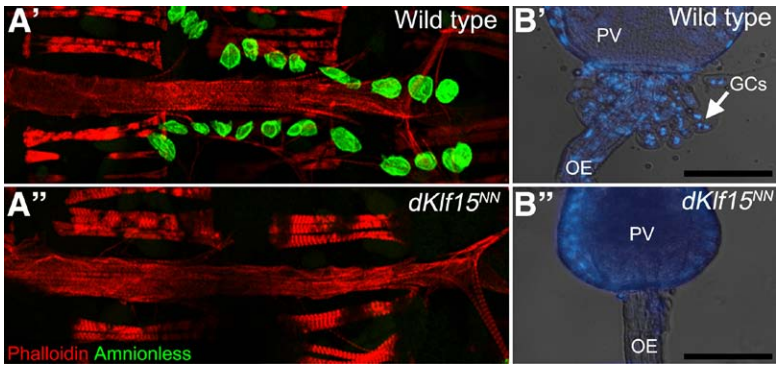

Figure 1. Loss of pericardial nephrocytes and garland cells in *dKlf15^{NN}* mutants. **A**, Adult control (*w^{1118}*; **A′**) and *dKlf15^{NN}* mutant flies (**A″**) were dissected and the heart fixed and stained with phalloidin to visualize the heart's actin cytoskeleton and antibodies to the pericardial nephrocyte marker Amnionless (*CG11592*). All pericardial nephrocytes fail to differentiate in the mutants, undergoing attrition during late larval development so that by adulthood there are none. **B**, Third instar larvae were dissected and the garland cells visualized after staining with Hoechst. In control flies (*w^{1118}*; **B′**) garland cells (GCs) are binucleate and situated at the interface between the proventriculus (PV) and esophagus (OE). In contrast, the garland cells fail to develop normally and are lost in the *dKlf15^{NN}* mutants (**B″**). Scale bar, 100 μm.

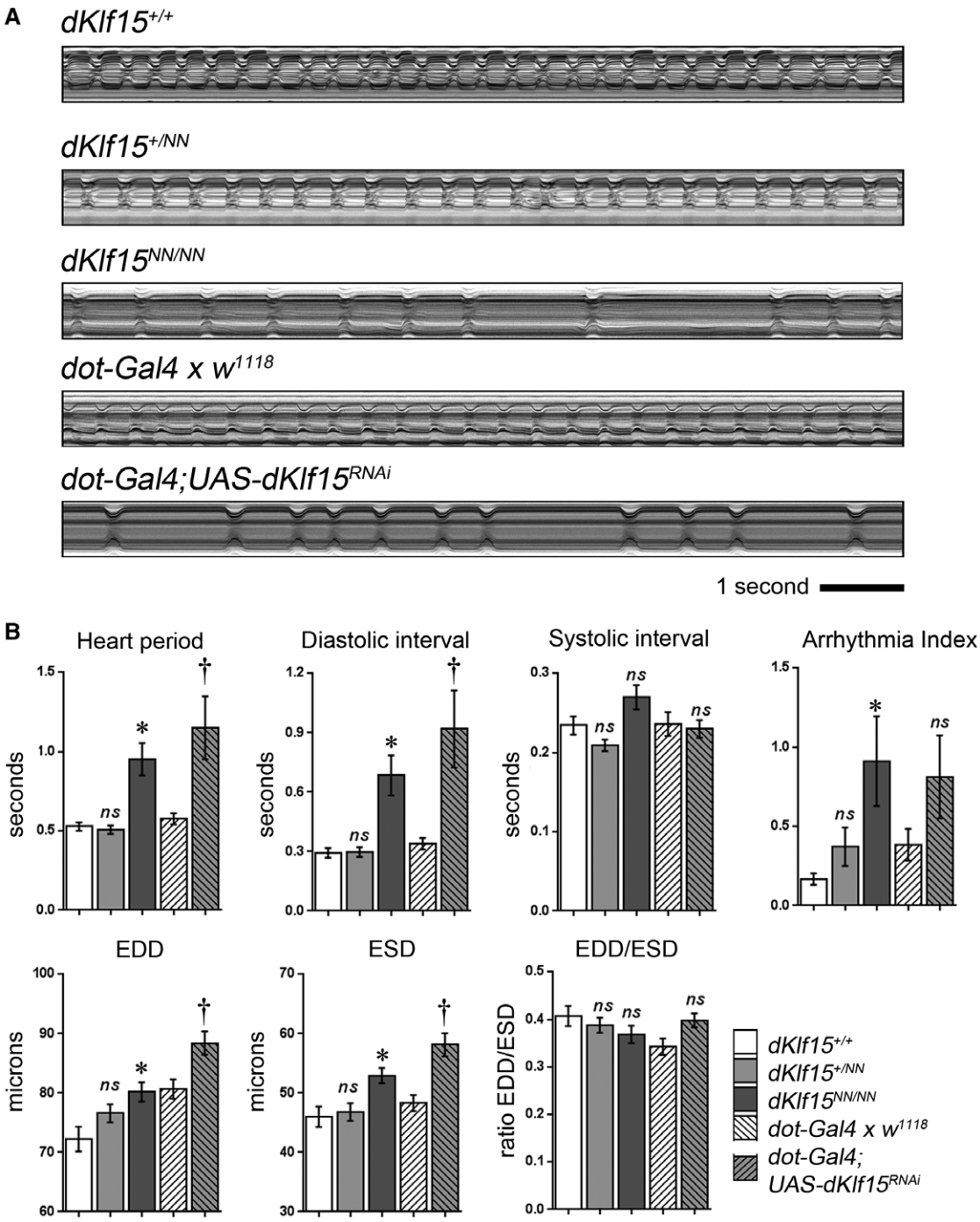

Figure 2. Loss of nephrocytes leads to cardiomyopathy. A, M-mode records of adult hearts. Regular contractions can be seen in wild-type (*dKlf15*$^{+/+}$), *dKlf15*$^{+/NN}$ heterozygote, and *dot-Gal4* outcrossed once to the *w*^{1118} control line (*dot-Gal4 x w*^{1118}); whereas flies homozygous for the *dKlf15*^{NN} allele, or in which *dKlf15* has been silenced in nephrocytes (*dot-Gal4; UAS-dKlf15*^{RNAi}), there is an abnormally long diastolic interval and periods of arrhythmia. **B**, Adult heart function. EDD indicates end-diastolic diameter; ESD, end-systolic diameter; and ns, not statistically different from *dKlf15*$^{+/+}$ or *dot* > *w*^{1118} control; **P*<0.01 compared with *dKlf15*$^{+/+}$; †*P*<0.01 compared with *dot* >*w*^{1118}); n=41 to 45 flies per genotype.

cause cardiomyopathy. Silencing *Amnionless* in nephrocytes did not cause nephrocyte death but did impair nephrocyte endocytic function (Figure 4A and 4B). Importantly, silencing *Amnionless* affected cardiac function by increasing the heart period because of a lengthening of the diastolic interval (Figure 4C), similar to the phenotype in *dKlf15* loss-of-function experiments.

Disruption of the Hemolymph Proteome in *dKlf15* Loss of Function Flies

Given that disruption of nephrocyte endocytosis was associated with the development of cardiomyopathy, it was hypothesized that nephrocytes may regulate levels of circulating, cardiomodulatory signals. We therefore examined the hemolymph proteome of control and *dKlf15*^{NN} mutants

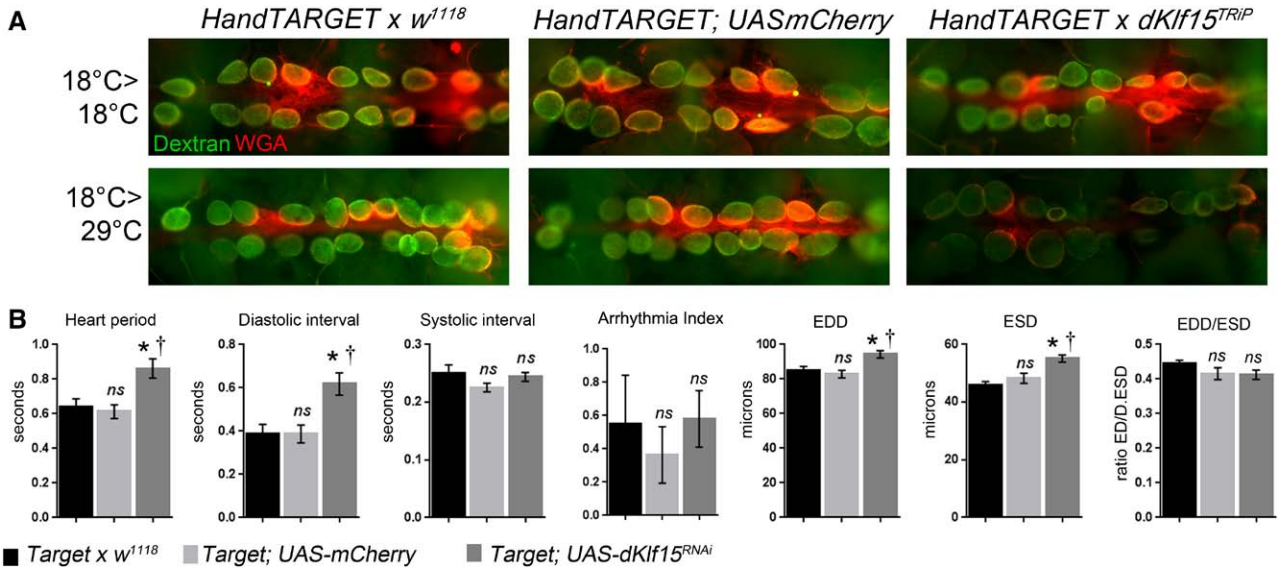

Figure 3. Conditional loss of nephrocyte function in adults leads to cardiomyopathy. *dKlf15* was conditionally silenced in the adult fly heart using the temperature-sensitive TARGET system driven by *Hand-Gal4*. Gene silencing is prevented at 18°C but permitted at higher temperatures (29°C). Flies were reared at 18°C until they eclosed and then maintained at this temperature to prevent gene silencing or moved to the higher temperature to allow *dKlf15* silencing. The *Hand-TARGET* parent line crossed to w^{1118} line or *UAS-mCherry* was used as controls. **A**, The endocytic function (ability to take-up fluorescently labeled dextran) was used to assess nephrocyte function. At the nonpermissive temperature, nephrocytes in all genotypes were able to accumulate dextran. When shifted to the permissive temperature the nephrocytes in control flies were still able to accumulate dextran, but flies in which *dKlf15* had been silenced could not. **B**, Quantification of heart function in adult flies reared at 18°C until eclosion and then transferred to 29°C for 2 weeks. The beating heart was imaged in semi-intact preparations using high frame rate video microscopy. n=20 for each genotype. EDD indicates end-diastolic interval; ESD, end-systolic diameter; and ns, not significantly different from Target or w^{1118}; * and †P<0.01 compared with Target, w^{1118} or Target; UAS mCherry controls, respectively.

using a method similar to that used by others to identify >700 larval hemolymph peptides.[30] Signals corresponding to 495 different proteins were identified. Of these, 209 were identified in the hemolymph of both genotypes, 192 were identified only in the control strain, and 94 were found only in $dKlf15^{NN}$ mutants (Figure 5A).

Proteins were allocated to 5 nonoverlapping groups (Table I in the Data Supplement); (group 1) unique to $dKlf15^{NN}$ mutants; (group 2) increased at least 2-fold in $dKlf15^{NN}$ mutants; (group 3) present in both genotypes and within 0.8- to 2-fold different in mutants relative to controls; (group 4) reduced by >0.8-fold in the mutants relative to controls; and (group 5) unique to controls.

It was predicted that ablation of the nephrocytes would lead to the accumulation of secreted proteins in circulation. To address this possibility, the SignalP 4.1 informatics tool was used to identify proteins predicted to have a signal peptide in their N-terminal region, a sequence associated with transport to the extracellular space.[27] Of the 448 proteins identified in the circulation of the reference strain, 39% were predicted to contain an N-terminal signal peptide (Figure 5B). In contrast, the hemolymph of the nephrocyte-free mutants was enriched for proteins predicted to contain a signal peptide (81%). In comparison with the total number of *Drosophila* genes predicted to encode signal peptides (3173 of 17 559 known genes, 18%), it was established that hemolymph proteome is enriched for proteins with signal peptides (P=3.827e-30), and that in the absence of nephrocytes, there is further enrichment for proteins with signal peptides compared with wild-type hemolymph (P=7.408e-35). These data are consistent with nephrocytes having a broad impact on the circulating proteome and suggest that loss of nephrocyte function causes the accumulation in the circulation of a large subset of secreted proteins.

Of the proteins found only in the $dKlf15^{NN}$ mutants (group 1), the most abundant signals were for the matricellular protein BM-40-SPARC (an ortholog of mammalian SPARC (Figures 5C, 5D, and 6A)[31]) and the cell adhesion protein DE-cadherin (encoded by shotgun, *shg*). Analysis of the SPARC peptide peak areas confirmed the absence of SPARC in the wild-type hemolymph (Figure I in the Data Supplement). Proteins significantly upregulated in the hemolymph of $dKlf15^{NN}$ mutants compared with wild-type flies (group 2; Figure 6B) included 3 genes with unknown functions (CG18067, CG15293, and CG14961; upregulated 27-, 9-, and 8.5-fold, respectively; P<0.05) as well as several proteins involved in immunity and clotting (gelsolin, immune-induced peptides 10 and 23 and the defence protein l(2)34F; P<0.05). The immune modulatory serpin necrotic[1] trended toward a 3-fold accumulation in the mutants' hemolymph.

Of the proteins common to both genotypes and at similar levels (group 3, Figure 6C), the largest spectral counts corresponded to the lipophorin, retinoid-binding and fatty acid–binding glycoprotein (*Rfabg*; spectral count of 2260±785 and 2097±570 for wild-type and mutant hemolymph; P=0.88) and the yolk proteins/vitellogenins (VIT 1, 2, and 3). Proteins with large spectral counts in the wild-types that were significantly downregulated in the mutants hemolymph (group 4; Figure 6D) included several intracellular cytoskeletal and

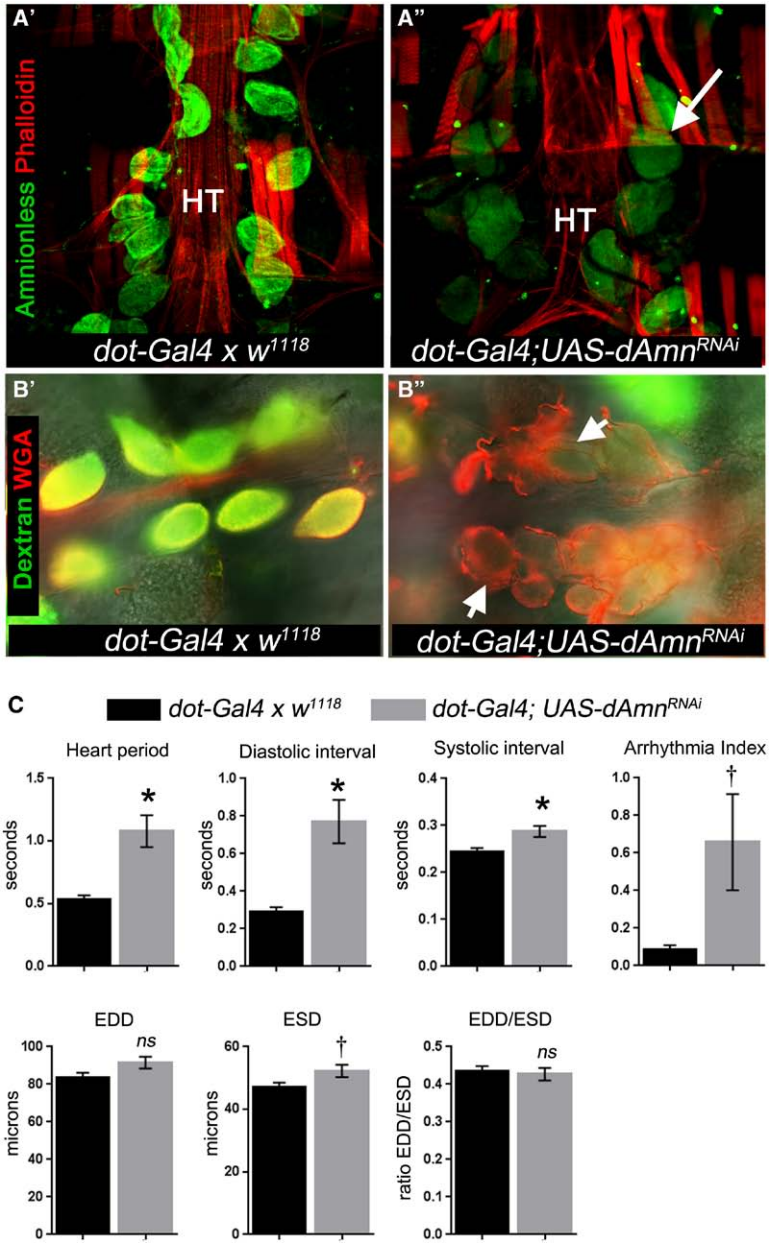

Figure 4. Loss of Amnionless function in nephrocytes leads to cardiomyopathy. **A**, *Amnionless* was silenced in nephrocytes using *dot-Gal4*. As a negative control, the parent driver line was outcrossed once to the w^{1118} line (*dot-Gal4 x* w^{1118}) and offspring analyzed. Micrographs show adult hearts stained with anti-Amnionless antibodies (green) and phalloidin (red). Amnionless protein was localized to nephrocytes in controls (**A′**), whereas silencing led to reduction in its detection but not the loss of pericardial nephrocytes (**A″**; arrow indicates a pericardial nephrocyte); HT indicates heart tube. **B**, Semi-intact heart preparations were incubated with fluorescently tagged 10-kDa dextran (green) and wheat germ agglutinin (red) for 30 minutes, washed and imaged. Arrows indicate nephrocytes. Dextran accumulated in controls (**B′**) but not in *Amnionless*-silenced nephrocytes (**B″**). WGA indicates wheat germ agglutinin. **C**, Quantification of heart function in flies with *Amnionless* silenced nephrocytes. Hearts were analyzed by high frame rate video microscopy of semi-intact adult heart preparations. EDD indicates end-diastolic interval; ESD, end-systolic diameter; EDD/ESD, fractional shortening of the heart contraction; and ns, not statistically different from control genotype (*dot-Gal4* x w^{1118}); **P*<0.01, †*<0.05; n=18 to 20 per genotype.

metabolic proteins (aldolase, enolase, and subunits of glyceraldehyde phosphate dehydrogenase enzyme). Finally, proteins unique to wild-type hemolymph (group 5, Figure 6E) included peroxiredoxin 5 (*Prdx5*; spectral count of 16±4 in wild-type and 2±1 in the mutant, $P<0.05$), iron regulatory protein 1B (*Irp1B*; spectral count of 22±6 in wild-type and 4±1 in mutant, $P<0.05$), and vacuolar H+ ATPase 68-kDa subunit 2A (*Vha68-2*; spectral count of 13±2 in wild-type, undetected in the mutant, $P<0.05$).

A $dSparc^{MI00329}$ Mutation Corrects the Cardiomyopathy in $dKlf15^{NN}$ Mutants

Of the proteins unique to the $dKlf15^{NN}$ mutants' hemolymph, SPARC was notable because of its role in collagen deposition and several growth factor signaling pathways thought to affect cardiac function.[32,33] We therefore tested whether *SPARC* contributed to the observed cardiomyopathy. We obtained a recessive lethal *Drosophila SPARC* allele ($dSparc^{MI00329}$) caused by the insertion of a 7.3-kb MiMIC transposon in the 5-prime untranscribed region of the *dSparc* open reading frame.[20] Homozygous adults do not develop, however, $dSparc^{MI00329}$ heterozygotes are viable, fertile, and develop to adulthood, albeit with *dSparc* gene expression reduced by 60% (Figure 7A). Homozygous $dKlf15^{NN}$ mutant females were crossed with males carrying the $dSparc^{MI00329}$ allele, and then the heart function of male progeny (ie, those hemizygous for $dKlf15^{NN}$ and heterozygous for the $dSparc^{MI00329}$ allele) was analyzed. It was found that the $dKlf15^{NN}$ mutant males had no nephrocytes and exhibited cardiomyopathy characterized by long diastolic intervals, similar to the phenotype of homozygous $dKlf15^{NN}$ mutant females (cf Figures 2 and 6). However, heart function parameters in $dSparc^{MI00329}$ heterozygotes (w^{1118}; $dSparc^{M100329}$) were not different from those of control w^{1118} flies, and specifically

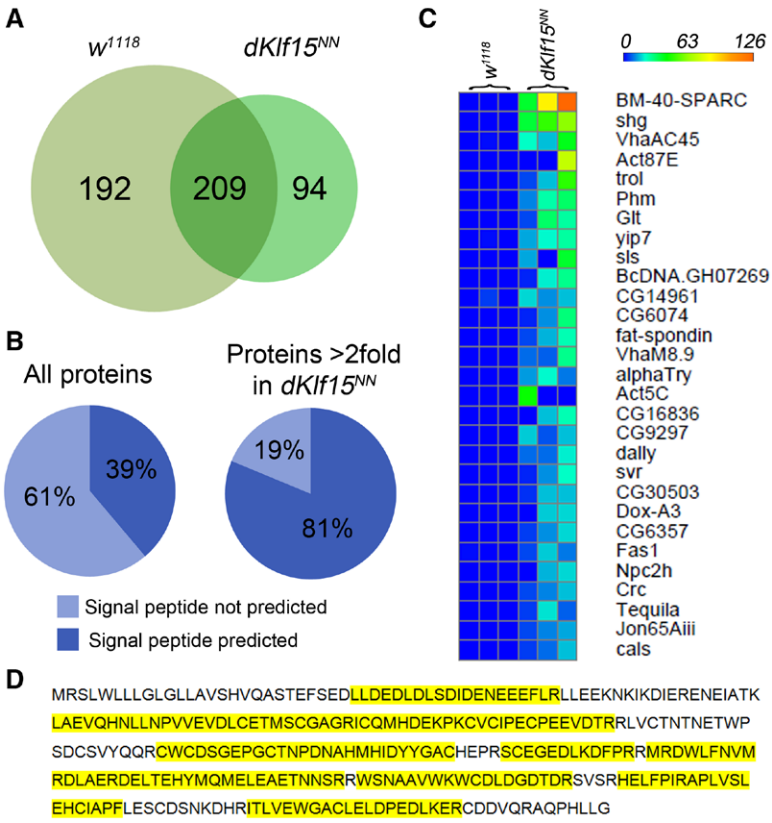

Figure 5. Proteomic analysis of adult *Drosophila* hemolymph. Hemolymph was collected from adult flies and the proteome analyzed. **A**, Number of different proteins identified in the hemolymph of adult control (w^{1118}) and mutant $dKlf15^{NN}$ flies. **B**, The number of proteins predicted to have a signal peptide by SignalP 4.1. **C**, Heat map showing a truncated list of proteins identified only in the hemolymph of $dKlf15^{NN}$ mutants. Proteins are rank ordered according to spectral count; each row represents 3 independent samples from each genotype (Table I in the Data Supplement). **D**, Coverage of secreted protein acidic and rich in cysteine (SPARC) protein sequence by detected peptides (yellow corresponds to regions detected in proteomics).

there was no increase in heart period/diastolic intervals as observed for hearts from hemizygous $dKlf15^{NN}$ mutants (Figure 7B). In contrast, when *Sparc* was silenced in wild-type cardiomyocytes, there was a significant impact on heart function (Figure II in the Data Supplement). Importantly, reducing *dSparc* expression rescued the abnormal heart phenotype in hemizygous $dKlf15^{NN}$ mutants (($dKlf15^{NN}$; $dSparc^{M100329+/-}$; Figure 7B), despite these flies having no nephrocytes. The findings demonstrate that heterozygosity for *SPARC* leading to reduced gene expression has no direct impact on cardiac function in the wild-type flies, whereas it ameliorates the cardiomyopathy caused by *Klf15*-induced loss of nephrocytes.

Discussion

The *Drosophila* heart model represents a highly tractable genetic system with which to study mammalian cardiac physiology. Although at an anatomic level the links between fly nephrocytes and cardiomyocytes may not be evolutionarily conserved, the high degree of gene conservation supports the use of this model for the identification of genetic pathways underlying human heart function. We used both proteomics and genetics to identify SPARC as an important component of cardiac function in *Drosophila*, highlighting the possibility that SPARC's role in the heart may be evolutionarily conserved from flies to humans. By using a cell-specific and temporally conditional nephrocyte loss of function paradigm, we establish that pericardial nephrocytes sustain normal heart function in adult *Drosophila*. Importantly, it was shown that nephrocytes prevent the development of a SPARC-dependent cardiomyopathy, a finding of considerable importance because SPARC is emerging as a clinically important target for the control of tissue fibrosis in humans.[33,34] Collectively, these findings highlight the importance of the *Drosophila* heart model as a means of identifying and studying cardiomodulatory signals of relevance to human cardiac function and suggest that changes to SPARC in humans may contribute to cardiac dysfunction in disease and aging.

Our data reaffirm that pericardial nephrocytes mediate noncell autonomous mechanisms controlling *Drosophila* heart function. The findings also suggest that the changes in heart morphology and the increased arrhythmias seen in $dKlf15^{NN}$ mutants were not only because of interactions between the cardiomyocytes and nephrocytes during pre-adult stages but also that adult heart rate is mediated by an on-going interaction between the cardiomyocytes and nephrocytes. Thus, it can be concluded that loss of nephrocytes or nephrocyte function both developmentally or acutely in adults, leads to cardiac dysfunction. Our data also suggest that the cardiomyopathy caused by loss of nephrocytes or nephrocyte function is linked to the nephrocytes' role in peripheral clearance.

To our knowledge, our data set represents the first examination of the adult *Drosophila* hemolymph proteome. The most abundant protein in the hemolymph of both wild-type and $dKlf15^{NN}$ mutants was Rfabg. Rfabg is a lipid transporter found in insect hemolymph and known to be required for Hedgehog and Wingless signaling.[35] There were also large signals for several important intracellular metabolic proteins (eg, aldolase, enolase, and subunits of the glyceraldehyde phosphate dehydrogenase enzyme). The presence of intracellular

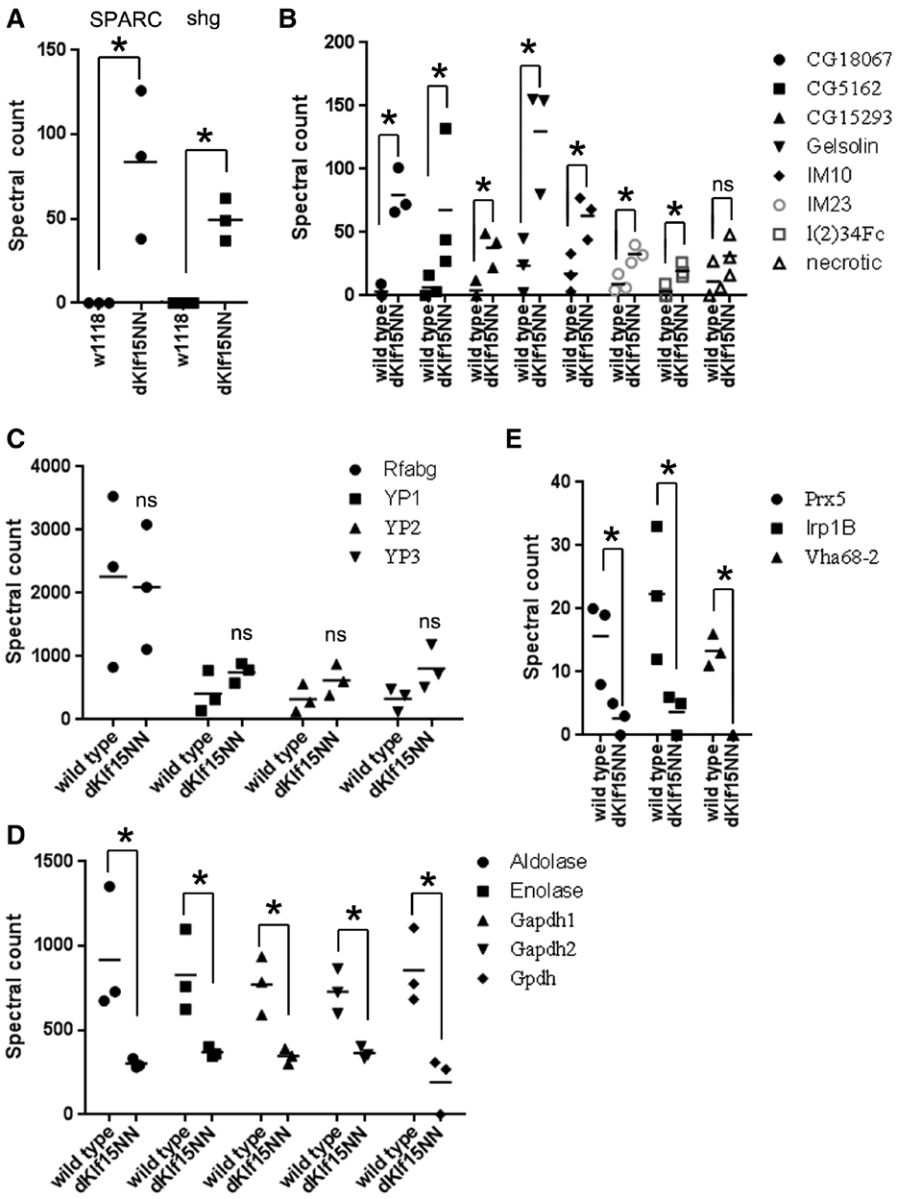

Figure 6. Mean spectral counts of hemolymph proteins. **A**, Counts for 2 most abundant proteins found only in the *dKlf15*^{NN} mutants hemolymph. **B**, Proteins showing an increase in the mutant's hemolymph. **C**, The most abundant proteins in the hemolymph of wild-type and *dKlf15*^{NN} mutants. **D**, Proteins significantly reduced in the hemolymph of the *dKlf15*^{NN} mutants. **E**, Proteins showing the largest, statistically significant, decrease in the mutant's hemolymph; n=3 independent hemolymph samples from ≈100 flies of each genotype; *P<0.05, ns indicates no significant difference. SPARC indicates secreted protein acidic and rich in cysteine.

proteins is a feature of the human plasma proteome, suggesting that intracellular proteins are a constituent of circulating fluids in animals. We also recorded an expected absence or near-absence from the adult hemolymph of the larval serum proteins LSP1α, LSP1β, LSP1γ, and LSP2, all of which are among the most highly represented proteins in larval hemolymph.[30] The LSPs are metabolized during the nonfeeding third instar and pupal stages, hence our data indicate that by the first week of adulthood, they are difficult to detect in the hemolymph.

In addition, there were proteins identified in both genotypes, which were significantly upregulated or downregulated in the hemolymph of *dKlf15*^{NN} mutants (group 2). The most highly upregulated signals were ascribed to genes with unknown functions (CG18067, CG15293, and CG14961) and proteins involved in immunity and clotting (gelsolin, immune-induced peptides 10 and 23, and the Defence protein l(2)34F). Although not reaching statistical significance, necrotic, an immune modulatory serpin removed from circulation by nephrocytes,[1] trended toward accumulating in the mutants' hemolymph of the mutants. In addition, there was a significant reduction in the mutants' hemolymph of peroxiredoxin 5, an antioxidant that also negatively regulates the immune response.[36] Collectively, these findings suggest that the mutant flies may have modified immune responses, and this is currently under investigation.

The most abundant proteins identified only in the hemolymph of the *dKlf15*^{NN} mutants were DE-cadherin and

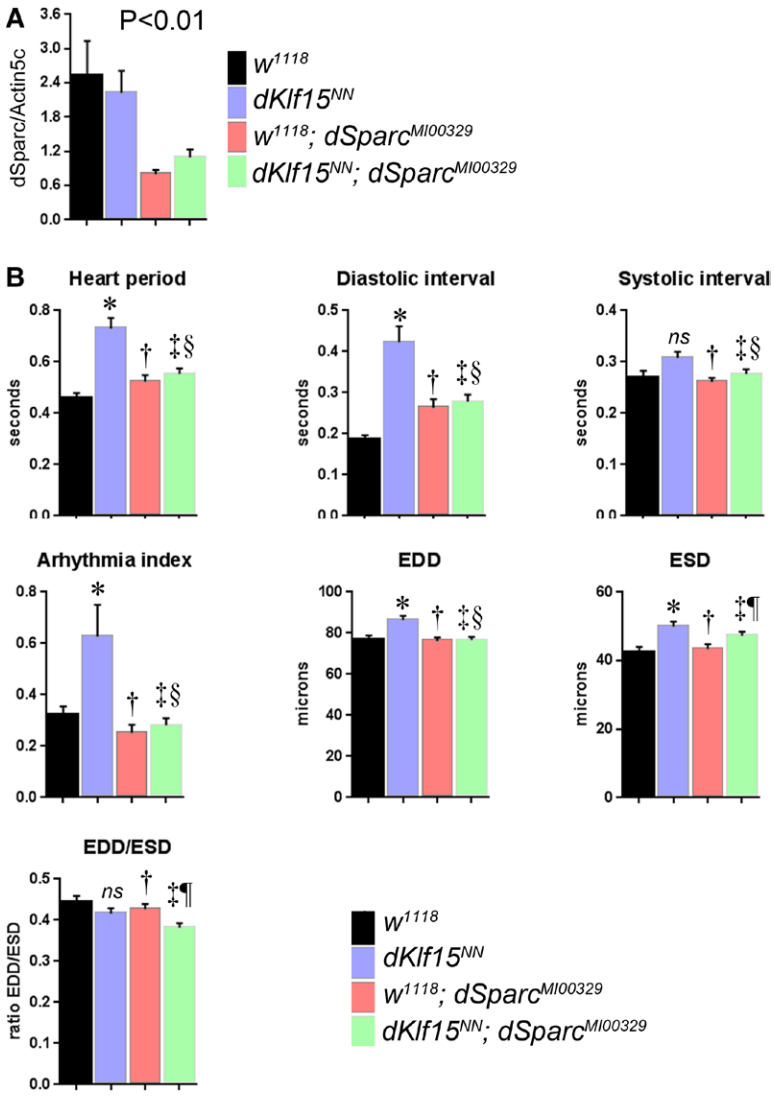

Figure 7. Secreted protein acidic and rich in cysteine (SPARC) mediates cardiomyopathy in *dKlf15*^{NN} mutants. The heart function of 2-week-old male flies of different genotypes was analyzed in semi-intact fly preparations using high frame rate videomicroscopy. Quantified data for several parameters are presented. EDD indicates end-diastolic diameter; and ESD, end-systolic diameter. *Different from *w*^{1118} (*P*<0.01); †Not different from *w*^{1118} (*P*>0.05); ‡Different from *dKlf15*^{NN} (*P*<0.01); §Not different from *w*^{1118}; *dSparc*^{MI00329} (*P*>0.05); ¶Not different from *dKlf15*^{NN} (*P*>0.05); ns, not different from *w*^{1118} (*P*>0.05); n=40 to 69 flies per genotype.

SPARC. DE-cadherin mediates cell adhesion and is critical for embryonic development and is present in the medulla of the lymph gland,[37] whereas SPARC stabilizes basal lamina by interacting with collagen IV, an interaction critical for normal development.[38,39] In contrast, the role of SPARC in postembryonic and adult *Drosophila* remains unclear. Mammalian SPARC directly binds to collagen as well as growth factors[40] and is associated with a diverse range of pathologies, including the maintenance of cardiac integrity[41] and metabolic syndrome.[42] Our data indicate that a SPARC-dependent cardiomyopathy is prevented in the *Drosophila* model via a nephrocyte-mediated clearance mechanism. Peripheral clearance of macromolecules is fundamentally important to tissue homeostasis but difficult to study in mammals. Although few studies exist, it is interesting to note that disruption of peripheral clearance by liver sinusoidal cells in stabilin-1 and stabilin-2 knockout mice led to local and systemic tissue fibrosis, albeit without an increase in circulating SPARC levels being detected.[43] It remains to be verified whether the increased SPARC levels directly cause cardiomyopathy or whether it is because of other hemolymph factors that are increased in *dKlf15*^{NN} mutants that act via a SPARC-dependent pathway.

Although abnormal cardiomyocyte function in *dKlf15*^{NN} mutants could be rescued by reducing *SPARC* gene dosage, we could not confirm whether this was an effect of reduced *SPARC* expression in the cardiomyocytes, because *SPARC* knockdown in wild-type cardiomyocytes led to a severe cardiomyopathy, characterized by reduced fractional shortening (Figure II in the Data Supplement). Hence, rescue of the cardiomyopathy by reducing *SPARC* gene dosage in the nephrocyte-free *dKlf15*^{NN} mutants may have been because of either a less severe reduction in *SPARC* expression in the cardiomyocytes or reduced *SPARC* expression in cells other than cardiomyocytes. Interestingly, moderate reductions in *ILK* expression in whole flies can extend lifespan and retard cardiac ageing, yet strong knockdown in cardiomyocytes has a profound negative impact on cardiac function.[8] Thus, different phenotypes can develop in the heart as a consequence of differing levels of gene silencing/gene dosage.

In summary, the *Drosophila* heart can develop a *SPARC*-dependent cardiomyopathy as a result of nephrocyte loss.

These findings identify *Drosophila* as a highly tractable model system with which to study the important relationship between tissue homeostasis and peripheral clearance, especially as it relates to human cardiac physiology. The next step will, therefore, be to establish how SPARC contributes to cardiac function in *Drosophila* and explore whether these mechanisms are conserved and relevant to the human heart.

Acknowledgments

Dr Hartley acknowledges support of the British Heart Foundation Centre of Research Excellence award (RE/08/001). Dr Hartley is especially grateful to Dr Georg Vogler and Ms. Hanah Catan (Sanford Burnham Medical Research Institute); Dr Richard Marley and Ms. Ashleigh Cheyne (University of Edinburgh) for comments and assistance with experiments. We thank the TRiP at Harvard Medical School (NIH/NIGMS R01-GM084947) for providing transgenic RNAi fly stocks used in this study.

Sources of Funding

Dr Hartley is supported by a British Heart Foundation Intermediate Basic Science Fellowship (FS/13/17/29905). This work was also supported by a British Heart Foundation Centre of Research Excellence award to the University of Edinburgh and by a subsistence grant from the Scottish Universities Life Science Alliance to Dr Hartley. This work was also supported by grants from the National Institutes of Health to R. Bodmer. K. Ocorr is supported by American Heart Association award 0835243N.

Disclosures

None.

References

1. Soukup SF, Culi J, Gubb D. Uptake of the necrotic serpin in *Drosophila melanogaster* via the lipophorin receptor-1. *PLoS Genet*. 2009;5:e1000532. doi: 10.1371/journal.pgen.1000532.
2. Das D, Aradhya R, Ashoka D, Inamdar M. Macromolecular uptake in Drosophila pericardial cells requires rudhira function. *Exp Cell Res*. 2008;314:1804–1810. doi: 10.1016/j.yexcr.2008.02.009.
3. Mills RP, King RC. The pericardial cells of *Drosophila melanogaster*. *Q J Microsc Sci*. 1965;106:261–268.
4. Neely GG, Kuba K, Cammarato A, Isobe K, Amann S, Zhang L, et al. A global *in vivo* Drosophila RNAi screen identifies NOT3 as a conserved regulator of heart function. *Cell*. 2010;141:142–153. doi: 10.1016/j.cell.2010.02.023.
5. Catterson JH, Heck MM, Hartley PS. Fermitins, the orthologs of mammalian Kindlins, regulate the development of a functional cardiac syncytium in *Drosophila melanogaster*. *PLoS One*. 2013;8:e62958. doi: 10.1371/journal.pone.0062958.
6. Viswanathan MC, Kaushik G, Engler AJ, Lehman W, Cammarato A. A *Drosophila melanogaster* model of diastolic dysfunction and cardiomyopathy based on impaired troponin-T function. *Circ Res*. 2014;114:e6–17. doi: 10.1161/CIRCRESAHA.114.302028.
7. Wessells RJ, Fitzgerald E, Cypser JR, Tatar M, Bodmer R. Insulin regulation of heart function in aging fruit flies. *Nat Genet*. 2004;36:1275–1281. doi: 10.1038/ng1476.
8. Nishimura M, Kumsta C, Kaushik G, Diop SB, Ding Y, Bisharat-Kernizan J, et al. A dual role for integrin-linked kinase and β1-integrin in modulating cardiac aging. *Aging Cell*. 2014;13:431–440. doi: 10.1111/acel.12193.
9. Birse RT, Choi J, Reardon K, Rodriguez J, Graham S, Diop S, et al. High-fat-diet-induced obesity and heart dysfunction are regulated by the TOR pathway in *Drosophila*. *Cell Metab*. 2010;12:533–544. doi: 10.1016/j.cmet.2010.09.014.
10. Na J, Musselman LP, Pendse J, Baranski TJ, Bodmer R, Ocorr K, et al. A *Drosophila* model of high sugar diet-induced cardiomyopathy. *PLoS Genet*. 2013;9:e1003175. doi: 10.1371/journal.pgen.1003175.
11. Na J, Sweetwyne MT, Park AS, Susztak K, Cagan RL. Diet-induced podocyte dysfunction in *Drosophila* and mammals. *Cell Rep*. 2015;12:636–647. doi: 10.1016/j.celrep.2015.06.056.
12. Buechling T, Akasaka T, Vogler G, Ruiz-Lozano P, Ocorr K, Bodmer R. Non-autonomous modulation of heart rhythm, contractility and morphology in adult fruit flies. *Dev Biol*. 2009;328:483–492. doi: 10.1016/j.ydbio.2009.02.013.
13. Fujioka M, Wessells RJ, Han Z, Liu J, Fitzgerald K, Yusibova GL, et al. Embryonic even skipped-dependent muscle and heart cell fates are required for normal adult activity, heart function, and lifespan. *Circ Res*. 2005;97:1108–1114. doi: 10.1161/01.RES.0000191546.08532.B2.
14. Johnson AN, Burnett LA, Sellin J, Paululat A, Newfeld SJ. Defective decapentaplegic signaling results in heart overgrowth and reduced cardiac output in *Drosophila*. *Genetics*. 2007;176:1609–1624. doi: 10.1534/genetics.107.073569.
15. Lim HY, Wang W, Chen J, Ocorr K, Bodmer R. ROS regulate cardiac function via a distinct paracrine mechanism. *Cell Rep*. 2014;7:35–44. doi: 10.1016/j.celrep.2014.02.029.
16. Das D, Aradhya R, Ashoka D, Inamdar M. Post-embryonic pericardial cells of Drosophila are required for overcoming toxic stress but not for cardiac function or adult development. *Cell Tissue Res*. 2008;331:565–570. doi: 10.1007/s00441-007-0518-z.
17. Ivy JR, Drechsler M, Catterson JH, Bodmer R, Ocorr K, Paululat A, et al. Klf15 is critical for the development and differentiation of *Drosophila* nephrocytes. *PLoS One*. 2015;10:e0134620. doi: 10.1371/journal.pone.0134620.
18. Frangogiannis NG. Matricellular proteins in cardiac adaptation and disease. *Physiol Rev*. 2012;92:635–688. doi: 10.1152/physrev.00008.2011.
19. Kimbrell DA, Hice C, Bolduc C, Kleinhesselink K, Beckingham K. The Dorothy enhancer has Tinman binding sites and drives hopscotch-induced tumor formation. *Genesis*. 2002;34:23–28. doi: 10.1002/gene.10134.
20. Venken KJ, Schulze KL, Haelterman NA, Pan H, He Y, Evans-Holm M, et al. MiMIC: a highly versatile transposon insertion resource for engineering *Drosophila melanogaster* genes. *Nat Methods*. 2011;8:737–743.
21. Sellin J, Albrecht S, Kölsch V, Paululat A. Dynamics of heart differentiation, visualized utilizing heart enhancer elements of the *Drosophila melanogaster* bHLH transcription factor hand. *Gene Expr Patterns*. 2006;6:360–375. doi: 10.1016/j.modgep.2005.09.012.
22. McGuire SE, Mao Z, Davis RL. Spatiotemporal gene expression targeting with the TARGET and gene-switch systems in *Drosophila*. *Sci STKE*. 2004;2004:pl6. doi: 10.1126/stke.2202004pl6.
23. Park SK, Venable JD, Xu T, Yates JR III. A quantitative analysis software tool for mass spectrometry-based proteomics. *Nat Methods*. 2008;5:319–322. doi: 10.1038/nmeth.1195.
24. Edelstein A, Amodaj N, Hoover K, Vale R, Stuurman N. Computer control of microscopes using μManager. *Curr Protoc Mol Biol*. 2010;Chapter 14:Unit14.20. doi: 10.1002/0471142727.mb1420s92.
25. Ocorr K, Reeves NL, Wessells RJ, Fink M, Chen HS, Akasaka T, et al. KCNQ potassium channel mutations cause cardiac arrhythmias in Drosophila that mimic the effects of aging. *Proc Natl Acad Sci U S A*. 2007;104:3943–3948. doi: 10.1073/pnas.0609278104.
26. Brill LM, Motamedchaboki K, Wu S, Wolf DA. Comprehensive proteomic analysis of Schizosaccharomyces pombe by two-dimensional HPLC-tandem mass spectrometry. *Methods*. 2009;48:311–319. doi: 10.1016/j.ymeth.2009.02.023.
27. Petersen TN, Brunak S, von Heijne G, Nielsen H. SignalP 4.0: discriminating signal peptides from transmembrane regions. *Nat Methods*. 2011;8:785–786. doi: 10.1038/nmeth.1701.
28. Halbritter F, Vaidya HJ, Tomlinson SR. GeneProf: analysis of high-throughput sequencing experiments. *Nat Methods*. 2012;9:7–8. doi: 10.1038/nmeth.1809.
29. Zhang F, Zhao Y, Chao Y, Muir K, Han Z. Cubilin and amnionless mediate protein reabsorption in *Drosophila* nephrocytes. *J Am Soc Nephrol*. 2013;24:209–216. doi: 10.1681/ASN.2012080795.
30. Handke B, Poernbacher I, Goetze S, Ahrens CH, Omasits U, Marty F, et al. The hemolymph proteome of fed and starved *Drosophila* larvae. *PLoS One*. 2013;8:e67208. doi: 10.1371/journal.pone.0067208.
31. Maurer P, Hohenadl C, Hohenester E, Göhring W, Timpl R, Engel J. The C-terminal portion of BM-40 (SPARC/osteonectin) is an autonomously folding and crystallisable domain that binds calcium and collagen IV. *J Mol Biol*. 1995;253:347–357. doi: 10.1006/jmbi.1995.0557.

32. de Castro Brás LE, Toba H, Baicu CF, Zile MR, Weintraub ST, Lindsey ML, et al. Age and SPARC change the extracellular matrix composition of the left ventricle. *Biomed Res Int*. 2014;2014:810562. doi: 10.1155/2014/810562.
33. Kos K, Wilding JP. SPARC: a key player in the pathologies associated with obesity and diabetes. *Nat Rev Endocrinol*. 2010;6:225–235. doi: 10.1038/nrendo.2010.18.
34. Trombetta-Esilva J, Bradshaw AD. The function of SPARC as a mediator of fibrosis. *Open Rheumatol J*. 2012;6:146–155. doi: 10.2174/1874312901206010146.
35. Panáková D, Sprong H, Marois E, Thiele C, Eaton S. Lipoprotein particles are required for Hedgehog and Wingless signalling. *Nature*. 2005;435:58–65. doi: 10.1038/nature03504.
36. Radyuk SN, Michalak K, Klichko VI, Benes J, Orr WC. Peroxiredoxin 5 modulates immune response in *Drosophil*a. *Biochim Biophys Acta*. 2010;1800:1153–1163. doi: 10.1016/j.bbagen.2010.06.010.
37. Jung SH, Evans CJ, Uemura C, Banerjee U. The *Drosophila* lymph gland as a developmental model of hematopoiesis. *Development*. 2005;132:2521–2533. doi: 10.1242/dev.01837.
38. Martinek N, Shahab J, Saathoff M, Ringuette M. Haemocyte-derived SPARC is required for collagen-IV-dependent stability of basal laminae in *Drosophila* embryos. *J Cell Sci*. 2008;121(pt 10):1671–1680. doi: 10.1242/jcs.021931.
39. Pastor-Pareja JC, Xu T. Shaping cells and organs in *Drosophila* by opposing roles of fat body-secreted collagen IV and perlecan. *Dev Cell*. 2011;21:245–256. doi: 10.1016/j.devcel.2011.06.026.
40. Bradshaw AD. Diverse biological functions of the SPARC family of proteins. *Int J Biochem Cell Biol*. 2012;44:480–488. doi: 10.1016/j.biocel.2011.12.021.
41. Schellings MW, Vanhoutte D, Swinnen M, Cleutjens JP, Debets J, van Leeuwen RE, et al. Absence of SPARC results in increased cardiac rupture and dysfunction after acute myocardial infarction. *J Exp Med*. 2009;206:113–123. doi: 10.1084/jem.20081244.
42. Tartare-Deckert S, Chavey C, Monthouel MN, Gautier N, Van Obberghen E. The matricellular protein SPARC/osteonectin as a newly identified factor up-regulated in obesity. *J Biol Chem*. 2001;276:22231–22237. doi: 10.1074/jbc.M010634200.
43. Schledzewski K, Géraud C, Arnold B, Wang S, Gröne HJ, Kempf T, et al. Deficiency of liver sinusoidal scavenger receptors stabilin-1 and -2 in mice causes glomerulofibrotic nephropathy via impaired hepatic clearance of noxious blood factors. *J Clin Invest*. 2011;121:703–714. doi: 10.1172/JCI44740.

CLINICAL PERSPECTIVE

In this work, we identified a genetic pathway in *Drosophila* linking cardiac function with the matricellular protein secreted protein acidic and rich in cysteine (SPARC). Changes to *SPARC* gene expression or protein levels in humans are associated with cardiac aging, chronic inflammatory disease, and metabolic syndrome. SPARC controls collagen deposition as well as mitogenic signaling and, as such, it is a potential clinical target with which to control scarring and organ dysfunction. It has been noted that *Drosophila* heart function is regulated by pericardial nephrocytes, highly endocytic kidney-like cells that flank the heart and filter the fly's blood. Our research aims to understand this relationship because the mechanisms involved may be relevant to the regulation of the human heart. To address this, we genetically ablated the nephrocytes and analyzed heart function as well as the blood proteome, in the hope of discovering cardiomodulatory peptides. We found that nephrocyte loss led to a severe cardiomyopathy, characterized by tissue remodeling and a slow, irregular heartbeat. Proteomics revealed an accumulation of many circulating proteins, most notably SPARC. We then conducted genetic loss of function experiments and established that the cardiomyopathy was dependent on *SPARC*. It remains to be seen whether this link involves SPARC's role in collagen deposition or a novel, uncharacterized mechanism. Nevertheless, by establishing a link between *SPARC* and cardiac function in *Drosophila* we now have a new, powerful tool in the research armoury with which to ascertain how *SPARC* contributes to cardiac function in humans.

SPARC–Dependent Cardiomyopathy in *Drosophila*

Paul S. Hartley, Khatereh Motamedchaboki, Rolf Bodmer and Karen Ocorr

Circ Cardiovasc Genet. 2016;9:119-129; originally published online February 2, 2016;
doi: 10.1161/CIRCGENETICS.115.001254
Circulation: Cardiovascular Genetics is published by the American Heart Association, 7272 Greenville Avenue, Dallas, TX 75231

Print ISSN: 1942-325X. Online ISSN: 1942-3268

SUPPLEMENTAL MATERIAL.

Supplemental Methods.

rtPCR

Total RNA was isolated from adult female flies using a Qiagen RNeasy Mini kit (Qiagen, Manchester, UK) according to the manufacturer's instructions. cDNA was prepared from 1 µg of total DNase-treated RNA by incubating the RNA with Oligo-dT primers at 65ºC for 10 min and then placing the reaction on ice for 5 min. Second strand synthesis was performed using Roche Expand RT (Roche Products Limited, Welwyn Garden City, UK). Quantitative PCR was then performed using 10 µL reaction volumes in 384-well format in a Roche LightCycler 480 Intron-spanning primers were used to determine the relative concentration of *Drosophila SPARC* (left, CGACATCGATGAGAACGAAG; right, TCGCGCTCAATATCCTTGAT), using *Actin5C* as a reference control. Quantified data are presented at the mean (+/-SEM) of six independent samples from wild type and *SPARC*-mutant flies.

Imaging the adult heart

Adults (2-3 week old unless stated otherwise) were anaesthetised with Flynap (Carolina Biological Supply Company, Burlington, NC, USA), dissected and hearts stained as described previously[1, 2]. For some experiments, vital dyes were used to identify functional nephrocytes or test their endocytic function (wheat germ agglutinin at 1µg / mL for 15 minutes or 50 µg / mL 10 kDa fluorescently labelled dextran for 0-30 minutes). Semi-intact preparations were then washed three times, fixed for 20 minutes with 1% formaldehyde and co-stained with antibodies (and then the relevant secondary antibodies) or Hoechst to visualise DNA and then imaged.

Epifluorescence microscopy of adult fly tissues

Semi-intact preparations were washed three times, fixed for 20 minutes with 1% formaldehyde, permeabilised with 0.1% TritonX-100 in phosphate buffered saline and co-stained with phalloidin (to visualise the actin cytoskeleton of the heart) and antibodies to the nephrocyte endocytosis protein Amnionless. To identify the

garland cells Hoechst 33342 was used to visualise DNA (garland cells having a binucleate nuclear morphology and distinct anatomical location at the interface between the oesophagus and paraventriculus). Fluoresce microscopy of flies was performed using a Zeiss LSM780 coupled to Zen image analysis software (Carl Zeiss, Welwyn Garden City, UK). Phase images were captured on a Zeiss Axiolab and images captured with an ORCA-ER CCD camera (Hamamatsu Photonics KK, Japan; Welwyn Garden City, UK) coupled to Openlab 4.1 (Improvision, Coventry, UK). Images were coloured, contrast enhanced and overlaid using Photoshop CS3. All micrographs were collected using the same microscope settings and image alterations, which were limited to contrast and brightness enhancement.

References.

1. Catterson JH, Heck MM, Hartley PS. Fermitins, the orthologs of mammalian kindlins, regulate the development of a functional cardiac syncytium in drosophila melanogaster. *PLoS One*. 2013;8:e62958.
2. Park SK, Venable JD, Xu T, Yates JR. A quantitative analysis software tool for mass spectrometry-based proteomics. *Nature Methods*. 2008;5:319-322.

Supplemental Figure S1.

SPARC peptide peak areas. Chromatograms for identified SPARC peptides are shown. In each panel the upper two chromatograms show peptide peaks from two technical replicates of a sample from the wild type (w^{1118}) hemolymph and the lower two chromatograms correspond to two technical replicates from a sample of the mutant ($dKlf15^{NN}$) hemolymph. In each case the peptide is detected in the mutant but not the wild type hemolymph.

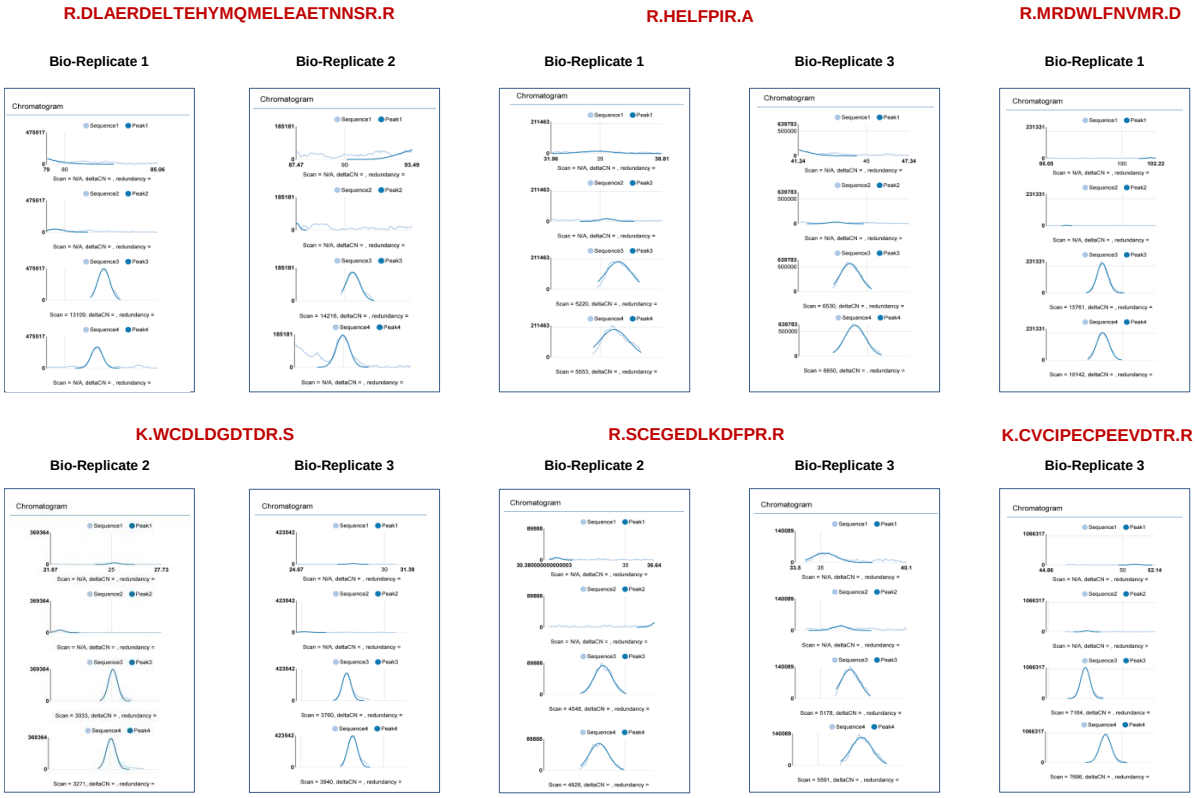

Supplemental Figure S2.

Effect of *SPARC* knock-down on heart function.

The function of the adult heart was analysed by high frame rate videomicroscopy (as described in the methods section of the main document). (A) The M-modes show the distance moved by the wall of the heart during a contraction (Fractional Shortening, red arrows). The control heart shows robust contraction between diastole to systole, whereas there is significantly less contraction when *SPARC* is silenced in the cardiomyocytes. (B) The graph shows the relative distance moved by the heart walls during diastole and systole (Fractional Shortening). The knock-down of *SPARC* in cardiomyocytes using the *TinCΔ4* driver (TinCd4 x Sparc TRiP) had a significant impact on fractional shortening that was not seen in either of the control genotypes (TinCd4 x w1118 and w1118 x Sparc TRiP). *n* = 19 to 29 flies per genotype. *P<0.001.

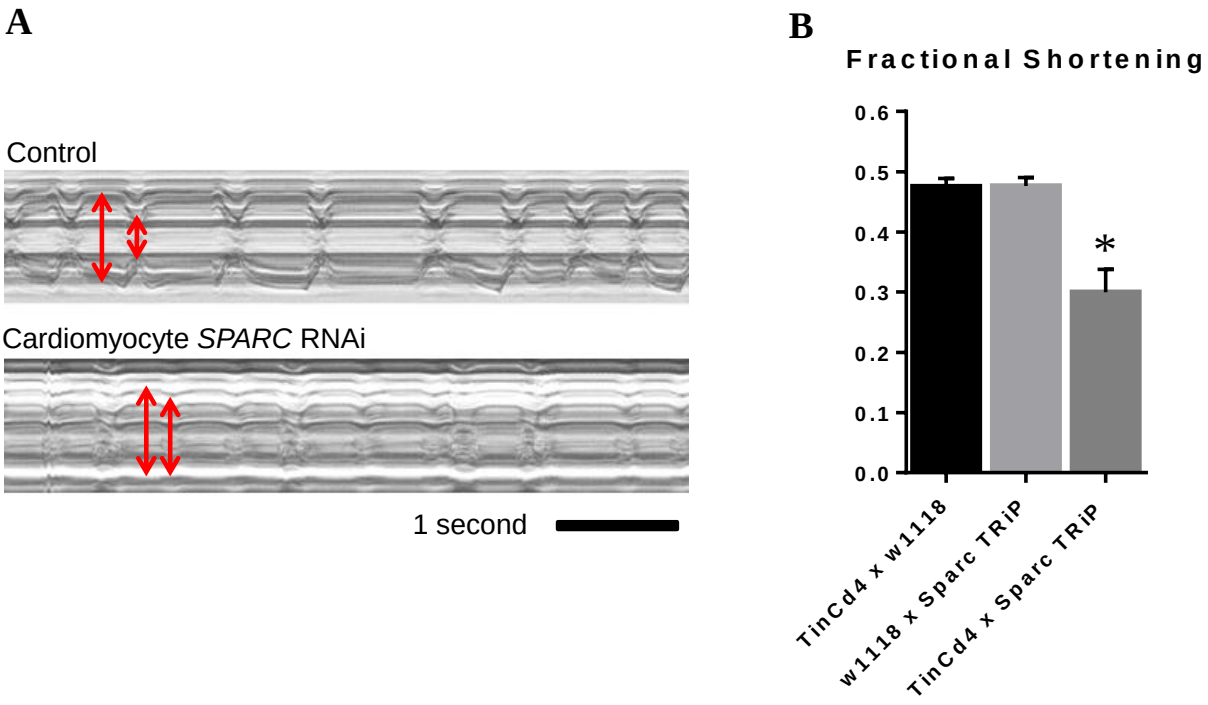

Supplemental Table. Proteomics Data

Group 1: Present in *dKlf15 ^{NN}* mutant but undetected in *w ^{1118}* control
(a mean of two spectral counts or lower was regarded as undetected)

	Uniprot ID	Annotation	w1118				dKlf15NN				w1118			dKlf15NN			
			#1	#2	#3		#1	#2	#3		Mean	SEM		Mean	SEM	t-Test	B-H Correction
tr|O97365|O97365_DROME	O97365	BM-40-SPARC	0	0	0		38	87	126		0	0		83	26	0.031	0.160
sp|Q24298|CADE_DROME	Q24298	shg	0	0	0		37	49	62		0	0		49	7	0.002	0.093
tr|Q7JR49|Q7JR49_DROME	Q7JR49	VhaAC45	0	1	0		22	16	40		0	0		26	7	0.023	0.143
sp|P10981|ACT5_DROME	P10981	Act87E	0	0	0		0	0	72		0	0		24	24	0.374	0.386
tr|A8JUV8|A8JUV8_DROME	A8JUV8	trol	0	0	0		6	16	48		0	0		23	13	0.135	0.266
sp|O01404|PHM_DROME	O01404	Phm	0	0	0		11	25	32		0	0		23	6	0.020	0.143
sp|P33438|GLT_DROME	P33438	Glt	0	0	0		6	32	26		0	0		21	8	0.057	0.216
tr|Q9VRS4|Q9VRS4_DROME	Q9VRS4	yip7	0	1	0		14	21	26		0	0		20	4	0.005	0.093
sp|Q9I7U4-1|TITIN_DROME	Q9I7U4	sls	0	0	0		14	0	38		0	0		17	11	0.197	0.327
tr|Q9VKG4|Q9VKG4_DROME	Q9VKG4	BcDNA.GH07269	0	0	0		3	20	28		0	0		17	7	0.080	0.266
tr|Q9VZQ7|Q9VZQ7_DROME	Q9VZQ7	CG14961	0	5	0		18	12	16		2	2		15	2	0.006	0.093
tr|Q9VB76|Q9VB76_DROME	Q9VB76	CG6074	0	0	0		3	12	30		0	0		15	8	0.129	0.266
tr|A1ZAP4|A1ZAP4_DROME	A1ZAP4	fat-spondin	0	0	0		6	15	24		0	0		15	5	0.042	0.178
tr|Q9VHG4|Q9VHG4_DROME	Q9VHG4	VhaM8.9	0	0	0		9	8	28		0	0		15	7	0.084	0.266
sp|P04814|TRYA_DROME	P04814	alphaTry	0	0	0		13	21	10		0	0		15	3	0.012	0.140
sp|P10987|ACT1_DROME	P10987	Act5C	0	0	0		43	0	0		0	0		14	14	0.374	0.386
tr|A1ZB62|A1ZB62_DROME	A1ZB62	CG16836	0	0	0		0	16	24		0	0		13	7	0.132	0.266
tr|Q8I0D4|Q8I0D4_DROME	Q8I0D4	CG9297	0	0	0		17	7	16		0	0		13	3	0.016	0.143
sp|Q24114|DALY_DROME	Q24114	dally	0	0	0		9	9	20		0	0		13	4	0.025	0.145
sp|P42787-1|CBPD_DROME	P42787	svr	0	0	0		3	12	22		0	0		12	5	0.084	0.266
tr|Q7JX94|Q7JX94_DROME	Q7JX94	CG30503	0	0	0		4	16	16		0	0		12	4	0.040	0.177
sp|Q9W1V6|PRPD3_DROME	Q9W1V6	Dox-A3	0	0	0		0	17	18		0	0		12	6	0.116	0.266
tr|A1Z9I0|A1Z9I0_DROME	A1Z9I0	CG6357	0	0	0		5	12	18		0	0		12	4	0.038	0.177
sp|P10674-1|FAS1_DROME	P10674	Fas1	1	0	0		6	17	10		0	0		11	3	0.027	0.148
tr|Q8IMH5|Q8IMH5_DROME	Q8IMH5	Npc2h	0	0	0		0	15	18		0	0		11	6	0.120	0.266
sp|P29413|CALR_DROME	P29413	Crc	0	0	0		6	11	16		0	0		11	3	0.023	0.143
tr|Q8IQB8|Q8IQB8_DROME	Q8IQB8	Tequila	0	0	0		5	19	8		0	0		10	4	0.067	0.240
tr|Q9VRS7|Q9VRS7_DROME	Q9VRS7	Jon65Aiii	0	0	0		6	11	14		0	0		10	2	0.014	0.143
sp|Q9V498|CSTN1_DROME	Q9V498	cals	0	0	0		5	9	16		0	0		10	3	0.037	0.177
sp|Q9VN93-1|CPR1_DROME	Q9VN93	CG12163	0	0	0		2	13	14		0	0		10	4	0.058	0.216
tr|Q9VMJ5|Q9VMJ5_DROME	Q9VMJ5	Gal	0	0	0		10	5	12		0	0		9	2	0.010	0.133
sp|O77150|IM02_DROME	O77150	IM2	0	0	0		0	0	26		0	0		9	9	0.374	0.386
tr|Q8MKJ5|Q8MKJ5_DROME	Q8MKJ5	CG30197	0	0	0		0	7	18		0	0		8	5	0.193	0.326
tr|Q8ING0|Q8ING0_DROME	Q8ING0	CG31326	0	4	0		6	19	0		1	1		8	6	0.301	0.386
tr|Q9VIQ5|Q9VIQ5_DROME	Q9VIQ5	CG10680	0	0	0		3	7	12		0	0		7	3	0.046	0.186
tr|Q7JYV3|Q7JYV3_DROME	Q7JYV3	CG12374	0	0	0		0	9	12		0	0		7	4	0.122	0.266
tr|Q8IRD6|Q8IRD6_DROME	Q8IRD6	Drsl4	0	0	2		0	5	16		1	1		7	5	0.246	0.369
sp|P13709-1|FSH_DROME	P13709	fs(1)h	0	0	0		21	0	0		0	0		7	7	0.374	0.386
tr|B7Z0T0|B7Z0T0_DROME	B7Z0T0	MP1	0	4	0		0	7	14		1	1		7	4	0.262	0.381
tr|Q9VJU6|Q9VJU6_DROME	Q9VJU6	NimB5	0	0	0		0	3	18		0	0		7	6	0.287	0.386
tr|Q9VN71|Q9VN71_DROME	Q9VN71	CG14661	0	0	0		5	7	8		0	0		6	1	0.002	0.093
tr|Q8SYQ4|Q8SYQ4_DROME	Q8SYQ4	CG31997	0	3	0		6	1	12		1	1		6	3	0.168	0.298
tr|Q9VZ66|Q9VZ66_DROME	Q9VZ66	CG15209	0	0	0		0	11	8		0	0		6	3	0.124	0.266
tr|A1Z7M8|A1Z7M8_DROME	A1Z7M8	Ance-4	0	0	0		6	8	4		0	0		6	1	0.006	0.093
sp|Q95029-1|CATL_DROME	Q95029	Cp1	0	0	0		0	7	10		0	0		6	3	0.132	0.266
tr|Q9VGK3|Q9VGK3_DROME	Q9VGK3	CG14715	0	0	0		3	5	8		0	0		6	1	0.017	0.143
tr|Q9VRT2|Q9VRT2_DROME	Q9VRT2	CG10472	0	0	0		0	4	12		0	0		5	4	0.205	0.334
sp|Q9VB11|UNC80_DROME	Q9VB11	CG18437	0	0	0		0	0	16		0	0		5	5	0.374	0.386
sp|Q9VW71|FAT2_DROME	Q9VW71	kug	0	0	0		0	0	16		0	0		5	5	0.374	0.386
tr|Q9VEP8|Q9VEP8_DROME	Q9VEP8	Irc	0	0	0		2	4	10		0	0		5	2	0.106	0.266
tr|Q86P15|Q86P15_DROME	Q86P15	ltl	0	0	0		5	11	0		0	0		5	3	0.170	0.298
tr|Q7JY07|Q7JY07_DROME	Q7JY07	CG9010	0	0	0		14	0	0		0	0		5	5	0.374	0.386
tr|Q9VAQ4|Q9VAQ4_DROME	Q9VAQ4	CG11841	0	5	0		1	5	8		2	2		5	2	0.347	0.386
tr|Q24485|Q24485_DROME	Q24485	RNaseX25	0	0	0		0	4	10		0	0		5	3	0.184	0.317
sp|Q9NB71|HIW_DROME	Q9NB71	hiw	0	0	0		0	0	14		0	0		5	5	0.374	0.386
tr|Q9VAY0|Q9VAY0_DROME	Q9VAY0	CG5527	0	3	0		3	3	8		1	1		5	2	0.123	0.266
tr|A8DY49|A8DY49_DROME	A8DY49	CG34215	0	0	0		0	3	10		0	0		4	3	0.231	0.358
tr|Q7JV39|Q7JV39_DROME	Q7JV39	CG11400	0	0	0		2	3	8		0	0		4	2	0.108	0.266
tr|Q9VQT6|Q9VQT6_DROME	Q9VQT6	CG3513	4	0	0		0	4	8		1	1		4	2	0.353	0.386
tr|Q7KTA1|Q7KTA1_DROME	Q7KTA1	NimB2	0	0	0		0	0	12		0	0		4	4	0.374	0.386
tr|Q9Y136|Q9Y136_DROME	Q9Y136	CG14526	0	4	0		2	9	0		1	1		4	3	0.452	0.457
tr|Q9W2F1|Q9W2F1_DROME	Q9W2F1	CG15674	0	0	0		6	4	2		0	0		4	1	0.021	0.143
tr|Q9VGE7|Q9VGE7_DROME	Q9VGE7	Ect3	0	0	0		6	0	6		0	0		4	2	0.117	0.266
tr|A1Z876|A1Z876_DROME	A1Z876	Ndg	0	0	0		5	7	0		0	0		4	2	0.127	0.266
tr|Q5BI82|Q5BI82_DROME	Q5BI82	CG13023	0	0	0		5	0	6		0	0		4	2	0.121	0.266
tr|Q9VIQ4|Q9VIQ4_DROME	Q9VIQ4	Hf	0	4	0		5	0	6		1	1		4	2	0.374	0.386
tr|Q8IHA8|Q8IHA8_DROME	Q8IHA8	CG8273	0	0	0		4	7	0		0	0		4	2	0.140	0.266
tr|Q9VFN7|Q9VFN7_DROME	Q9VFN7	Npc2b	0	0	0		2	4	4		0	0		3	1	0.003	0.093
tr|A1Z6H6|A1Z6H6_DROME	A1Z6H6	CG7791	0	0	0		0	0	10		0	0		3	3	0.374	0.386
tr|Q8MMD2|Q8MMD2_DROME	Q8MMD2	Eps-15	0	0	0		0	0	10		0	0		3	3	0.374	0.386
tr|Q9W1H6|Q9W1H6_DROME	Q9W1H6	CG5597	0	4	0		0	4	6		1	1		3	2	0.417	0.426
tr|Q7K088|Q7K088_DROME	Q7K088	Obp56e	0	3	0		10	0	0		1	1		3	3	0.525	0.525
tr|Q23995|Q23995_DROME	Q23995	tok	0	0	0		0	1	8		0	0		3	2	0.277	0.386
sp|P33450|FAT_DROME	P33450	ft	0	0	0		0	9	0		0	0		3	3	0.374	0.386
tr|A8JR58|A8JR58_DROME	A8JR58	CG5630	0	0	0		0	9	0		0	0		3	3	0.374	0.386
sp|Q9VEG6|PERC_DROME	Q9VEG6	Pxt	0	0	0		4	5	0		0	0		3	2	0.124	0.266
tr|Q95RA9|Q95RA9_DROME	Q95RA9	CG9796	0	0	0		3	0	6		0	0		3	2	0.152	0.283
tr|Q9W314|Q9W314_DROME	Q9W314	Ser7	0	0	0		2	7	0		0	0		3	2	0.242	0.369
tr|Q0E8P5|Q0E8P5_DROME	Q0E8P5	CG5758-RC	0	0	0		4	4	0		0	0		3	1	0.116	0.266
tr|Q9VV46|Q9VV46_DROME	Q9VV46	Cpr72Ec	0	0	0		0	4	4		0	0		3	1	0.116	0.266
tr|Q95SC0|Q95SC0_DROME	Q95SC0	CG9917-RA	0	0	0		0	8	0		0	0		3	3	0.374	0.386
tr|Q9VQ27|Q9VQ27_DROME	Q9VQ27	CG14352	0	0	0		0	8	0		0	0		3	3	0.374	0.386
tr|E1JI59|E1JI59_DROME	E1JI59	siz	0	0	0		0	0	8		0	0		3	3	0.374	0.386
tr|O77273|O77273_DROME	O77273	EG:66A1.2	0	0	0		0	0	8		0	0		3	3	0.374	0.386
tr|Q9VED8|Q9VED8_DROME	Q9VED8	DNaseII	0	0	0		0	0	8		0	0		3	3	0.374	0.386
tr|Q9VWT7|Q9VWT7_DROME	Q9VWT7	CG15043	0	0	0		2	5	0		0	0		3	2	0.170	0.298
sp|Q0KHY3-1|Y1004_DROME	Q0KHY3-1	mesh	0	0	0		0	1	6		0	0		2	2	0.250	0.369
tr|Q23984|Q23984_DROME	Q9VMD9	tig	0	0	0		2	5	0		0	0		2	2	0.217	0.342
tr|Q95SI9|Q95SI9_DROME	Q95SI9	CG3868	0	0	0		2	5	0		0	0		2	2	0.217	0.342
tr|Q9XZ34|Q9XZ34_DROME	Q9XZ34	Rif1	0	0	0		0	7	0		0	0		2	2	0.374	0.386
tr|Q8T4A8|Q8T4A8_DROME	Q8T4A8	CG7542	0	0	0		0	3	4		0	0		2	1	0.132	0.266
sp|Q70PY2|PGSB1_DROME	Q70PY2	PGRP-SB1	0	0	0		2	4	0		0	0		2	1	0.140	0.266
tr|A1Z8Q2|A1Z8Q2_DROME	A1Z8Q2	CG13185	0	0	0		6	0	0		0	0		2	2	0.374	0.386

Group 2: In both *w ^{1118}* and mutant but > 2-fold greater in *dKlf15 ^{NN}* mutant

	Uniprot ID	Annotation	w1118	dKlf15NN	w1118	dKlf15NN

			#1	#2	#3	#1	#2	#3	Mean	SEM	Mean	SEM	Fold chang	t-Test	B-H Correction
tr|A1ZBU8|A1ZBU8_DROME	A1ZBU8	CG18067	0	9	0	66	101	72	3	3	80	11	25.6	0.003	0.159
tr|Q8SXG0|Q8SXG0_DROME	Q8SXG0	CG5162	3	16	0	27	44	132	6	5	68	32	10.7	0.135	0.247
tr|Q9V3Y7|Q9V3Y7_DROME	Q9V3Y7	CG15293	0	12	0	22	49	42	4	4	38	8	9.5	0.019	0.172
sp|P54192|PBP2_DROME	P54192	Pbprp2	2	12	8	22	71	86	7	3	59	19	8.0	0.057	0.183
tr|Q7JYZ0|Q7JYZ0_DROME	Q7JYZ0	CG6426	0	7	0	8	17	26	2	2	17	5	7.7	0.058	0.183
tr|Q7KMM4|Q7KMM4_DROME	Q7KMM4	BcDNA.GH04962	0	8	0	12	17	24	3	3	18	3	6.7	0.026	0.172
sp|Q9V3Y3|DFP_DROME	Q9V3Y3	l(2)34Fc	0	9	0	18	15	26	3	3	20	3	6.3	0.022	0.172
tr|Q9W227|Q9W227_DROME	Q9W227	CG2852	5	17	10	39	52	106	11	4	66	20	6.1	0.057	0.183
sp|Q07171-1|GELS_DROME	Q07171	Gel	2	45	24	80	155	154	24	12	130	25	5.4	0.019	0.172
tr|Q8SYB5|Q8SYB5_DROME	Q8SYB5	Jon65Aiv	0	0	10	11	16	24	3	3	17	4	5.1	0.052	0.183
tr|Q7K533|Q7K533_DROME	Q7K533	CG11395	3	23	0	22	60	46	9	7	43	11	5.0	0.063	0.183
tr|Q9VH37|Q9VH37_DROME	Q9VH37	CG12811	1	5	0	4	7	20	2	2	10	5	4.5	0.201	0.266
tr|Q0KI00|Q0KI00_DROME	Q0KI00	SP1029	6	5	0	9	32	8	4	2	16	8	4.3	0.197	0.266
tr|Q7K084|Q7K084_DROME	Q7K084	Obp44a	5	12	6	23	31	46	8	2	33	7	4.3	0.022	0.172
tr|Q9W0J9|Q9W0J9_DROME	Q9W0J9	CG9119	1	8	0	5	13	20	3	2	13	4	4.0	0.131	0.247
sp|P29746|BNB_DROME	P29746	bnb	9	16	22	30	64	90	16	4	61	17	3.9	0.064	0.183
tr|Q9VCJ8|Q9VCJ8_DROME	Q9VCJ8	SPE	0	11	0	5	19	18	4	4	14	5	3.9	0.149	0.255
sp|Q9W1C9|PEB3_DROME	Q9W1C9	PebIII	2	13	18	22	45	62	11	5	43	12	3.8	0.065	0.183
tr|Q8INW9|Q8INW9_DROME	Q8INW9	fon	5	21	8	32	27	68	12	5	42	13	3.7	0.092	0.212
sp|Q8ML70-1|IM10_DROME	Q8ML70-1	IM10	3	33	16	44	77	68	17	9	63	10	3.6	0.026	0.172
sp|Q9V8F5|IM23_DROME	Q9V8F5	IM23	4	17	6	26	40	32	9	4	33	4	3.5	0.014	0.172
sp|Q06521|VTU3_DROME	Q06521	Vm34Ca	0	8	0	6	8	12	3	3	9	2	3.2	0.146	0.255
tr|Q8MYW6|Q8MYW6_DROME	Q8MYW6	CG17109	0	11	0	5	13	16	4	4	11	3	3.2	0.186	0.266
tr|Q9NF33|Q9NF33_DROME	Q9NF33	EG:103E12.2	7	36	6	33	60	50	16	10	48	8	2.9	0.069	0.183
tr|O97355|O97355_DROME	O97355	Tsf1	82	372	88	328	605	642	181	96	525	99	2.9	0.067	0.183
tr|Q7JWX3|Q7JWX3_DROME	Q7JWX3	nec	6	27	0	30	48	16	11	8	31	9	2.9	0.169	0.259
tr|Q8SY60|Q8SY60_DROME	Q8SY60	CG9928	6	31	24	38	53	82	20	7	58	13	2.9	0.063	0.183
tr|Q86BI9|Q86BI9_DROME	Q86BI9	CG18135	2	39	0	23	47	42	14	13	37	7	2.7	0.177	0.261
tr|Q9NFV5|Q9NFV5_DROME	Q9NFV5	Tep4	9	63	28	54	112	102	33	16	89	18	2.7	0.079	0.199
tr|Q9W306|Q9W306_DROME	Q9W306	CG9691	0	8	0	4	9	8	3	3	7	2	2.7	0.226	0.289
tr|A1ZAU4|A1ZAU4_DROME	A1ZAU4	CG4847-RD	0	11	0	3	15	10	4	4	9	3	2.6	0.304	0.330
tr|Q8IN51|Q8IN51_DROME	Q8IN51	CG31205-RB	10	35	26	30	61	88	24	7	60	17	2.5	0.116	0.246
sp|Q10714|ACE_DROME	Q10714	Ance	0	13	0	9	19	6	4	4	11	4	2.5	0.317	0.336
tr|Q8SZN1|Q8SZN1_DROME	Q8SZN1	CG31313	1	17	0	11	16	20	6	6	16	3	2.5	0.196	0.266
tr|A1Z7H7|A1Z7H7_DROME	A1Z7H7	CG8586-RA	0	16	0	10	17	12	5	5	13	2	2.5	0.240	0.289
sp|P06607|VIT3_DROME	P06607	Yp3	122	479	380	510	719	1184	327	106	804	199	2.5	0.102	0.225
sp|Q8MLZ7|IDGF3_DROME	Q8MLZ7	Idgf3	1	29	0	16	36	22	10	10	25	6	2.5	0.266	0.313
tr|Q7K127|Q7K127_DROME	Q7K127	CG7997	4	24	0	11	35	24	9	7	23	7	2.5	0.240	0.289
sp|Q9VU58|NPLP2_DROME	Q9VU58	Nplp2	65	328	148	226	405	694	180	78	442	136	2.5	0.171	0.259
tr|A1ZB61|A1ZB61_DROME	A1ZB61	CG15067	14	21	22	28	56	56	19	3	47	9	2.4	0.047	0.183
tr|Q9Y141|Q9Y141_DROME	Q9Y141	BcDNA.GH05741	1	13	0	4	16	16	5	4	12	4	2.4	0.291	0.330
tr|Q9VA42|Q9VA42_DROME	Q9VA42	Npc2g	10	41	28	30	83	78	27	9	63	17	2.4	0.127	0.247
tr|Q8IPH4|Q8IPH4_DROME	Q8IPH4	Tep2	7	39	4	28	37	52	17	11	39	7	2.3	0.161	0.259
sp|Q868Z9-1|PPN_DROME	Q868Z9	Ppn	4	65	28	30	60	138	33	18	76	32	2.3	0.301	0.330
tr|Q9VKR8|Q9VKR8_DROME	Q9VKR8	CG17108	16	13	14	50	7	44	14	1	33	13	2.3	0.230	0.289
tr|Q9VJQ3|Q9VJQ3_DROME	Q9VJQ3	yellow-c	2	9	12	11	21	20	8	3	18	3	2.2	0.089	0.212
tr|Q8IPB7|Q8IPB7_DROME	Q8IPB7	LM408	13	96	50	76	117	152	53	24	115	22	2.2	0.129	0.247
tr|A1ZBU5|A1ZBU5_DROME	A1ZBU5	CG13422	1	5	0	2	11	0	2	2	4	3	2.1	0.557	0.568
tr|Q9VI09|Q9VI09_DROME	Q9VI09	CG17919	0	24	4	10	23	26	9	7	20	5	2.1	0.305	0.330
tr|Q9VAI9|Q9VAI9_DROME	Q9VAI9	Obp99c	31	84	36	82	115	116	50	17	104	11	2.1	0.055	0.183
sp|Q9VLJ6|ACER_DROME	Q9VLJ6	Acer	4	73	12	26	72	84	30	22	61	18	2.0	0.332	0.345
tr|Q0E9C3|Q0E9C3_DROME	Q0E9C3	Sod3	0	11	0	0	5	16	4	4	7	5	2.0	0.579	0.579
tr|Q9VD48|Q9VD48_DROME	Q9VD48	CG5791	0	9	6	8	11	12	5	3	10	1	2.0	0.161	0.259

Group 3: In both w^{1118} and mutant and within >0.8 and <2-fold difference

	Uniprot ID	Annotation	w1118			dKlf15NN			w1118		dKlf15NN				
			#1	#2	#3	#1	#2	#3	Mean	SEM	Mean	SEM	Fold chang	t-Test	B-H Correction
sp|Q9VAI6|OB99B_DROME	Q9VAI6	Obp99b	10	24	36	31	16	90	23	7	46	23	1.9	0.402	1.000
sp|P02844|VIT2_DROME	P02844	Yp2	128	565	274	385	601	876	322	129	621	142	1.9	0.195	1.000
tr|Q9VKV2|Q9VKV2_DROME	Q9VKV2	CG5322	2	13	0	10	11	8	5	4	10	1	1.9	0.345	1.000
sp|P02843|VIT1_DROME	P02843	Yp1	143	775	316	578	784	886	411	188	749	91	1.8	0.181	1.000
tr|Q9VG08|Q9VG08_DROME	Q9VG08	yellow-f2	4	21	0	12	17	16	8	7	15	2	1.8	0.375	1.000
tr|Q9VME1|Q9VME1_DROME	Q9VME1	CG42369	2	16	0	3	9	20	6	5	11	5	1.8	0.534	1.000
tr|Q8SY86|Q8SY86_DROME	Q8SY86	CG16704	0	11	10	2	15	20	7	3	12	5	1.8	0.466	1.000
tr|Q7JQR3|Q7JQR3_DROME	Q7JQR3	CG4670	0	12	0	5	8	8	4	4	7	1	1.7	0.518	1.000
tr|Q86PE8|Q86PE8_DROME	Q86PE8	CG5390	7	25	8	15	25	30	14	6	24	4	1.7	0.247	1.000
tr|Q9VZ24|Q9VZ24_DROME	Q9VZ24	CG15201	0	3	6	2	5	8	3	2	5	2	1.7	0.457	1.000
tr|Q94881|Q94881_DROME	Q94881	Lectin-galC1	7	24	18	17	29	36	16	5	27	6	1.7	0.215	1.000
tr|A1Z6V5|A1Z6V5_DROME	A1Z6V5	Spn43Ab	4	40	26	19	51	44	23	11	38	10	1.6	0.360	1.000
sp|Q8IN44|TOTA_DROME	Q8IN44	TotA	4	77	16	36	55	62	32	23	51	8	1.6	0.484	1.000
sp|Q9V8Y2|OB56A_DROME	Q9V8Y2	Obp56a	2	29	8	14	19	28	13	8	20	4	1.5	0.478	1.000
sp|P08144|AMYA_DROME	P08144	Amy-p	0	53	20	11	43	54	24	16	36	13	1.5	0.598	1.000
tr|Q27598|Q27598_DROME	Q27598	1	46	109	92	70	132	160	82	19	121	27	1.5	0.309	1.000
sp|Q9V521|PRPA3_DROME	Q9V521	proPo-A3	50	185	102	82	173	232	112	39	162	44	1.4	0.445	1.000
sp|P23779|CYTL_DROME	P23779	Cys	27	103	102	70	107	154	77	25	110	24	1.4	0.401	1.000
tr|Q0E8C8|Q0E8C8_DROME	Q0E8C8	Spn77Ba	5	20	0	22	8	6	8	6	12	5	1.4	0.678	1.000
tr|Q7K3E2|Q7K3E2_DROME	Q7K3E2	CG5080	22	111	18	58	72	82	50	30	71	7	1.4	0.547	1.000
sp|P08171|EST6_DROME	P08171	Est-6	24	173	72	56	151	172	90	44	126	36	1.4	0.555	1.000
tr|Q2QBM1|Q2QBM1_DROME	Q2QBM1	Men	7	27	14	19	23	18	16	6	20	1	1.3	0.526	1.000
sp|P41572|6PGD_DROME	P41572	Pgd	4	0	6	2	7	4	3	2	4	1	1.2	0.713	1.000
sp|P82705|IM04_DROME	P82705	IM4	19	45	22	27	47	32	29	8	35	6	1.2	0.553	1.000
sp|Q8IN43|TOTC_DROME	Q8IN43	TotC	0	47	16	12	33	30	21	14	25	7	1.2	0.795	1.000
tr|Q9VTC3|Q9VTC3_DROME	Q9VTC3	CG6409	17	128	100	29	105	156	82	33	97	37	1.2	0.778	1.000
sp|Q9VAJ4|OB99A_DROME	Q9VAJ4	Obp99a	0	21	0	3	8	14	7	7	8	3	1.2	0.876	1.000
tr|A5XCL5|A5XCL5_DROME	A5XCL5	UGP	0	0	86	39	36	26	29	29	34	4	1.2	0.870	1.000
tr|Q76NR6|Q76NR6_DROME	Q76NR6	regucalcin	44	56	58	49	60	76	53	4	62	8	1.2	0.378	1.000
tr|Q9VBJ6|Q9VBJ6_DROME	Q9VBJ6	CG14540	0	0	12	0	0	14	4	4	5	5	1.2	0.919	1.000
sp|Q9V3D4|IDGF2_DROME	Q9V3D4	Idgf2	3	57	22	14	36	46	27	16	32	10	1.2	0.823	1.000
sp|Q8SY61|OB56D_DROME	Q8SY61	Obp56d	18	105	36	37	81	62	53	27	60	13	1.1	0.826	1.000
sp|Q23997|CH47_DROME	Q23997	CG5210	48	243	88	93	164	164	126	59	140	24	1.1	0.836	1.000
tr|Q9VQT8|Q9VQT8_DROME	Q9VQT8	CG16712	49	156	98	68	97	170	101	31	112	30	1.1	0.813	1.000
tr|Q0E9F9|Q0E9F9_DROME	Q0E9F9	CG2915-RB	4	21	10	5	17	16	12	5	13	4	1.1	0.883	1.000
tr|Q7KTG2|Q7KTG2_DROME	Q7KTG2	Apoltp	0	25	0	5	11	12	8	8	9	2	1.1	0.939	1.000
tr|Q9VVP9|Q9VVP9_DROME	Q9VVP9	CG4306	0	7	0	3	4	0	2	2	2	1	1.1	0.947	1.000
tr|Q7JYH0|Q7JYH0_DROME	Q7JYH0	CG6503	17	96	40	15	29	116	51	23	54	32	1.0	0.953	1.000
tr|B7YZV3|B7YZV3_DROME	B7YZV3	Pde1c	3	23	8	3	12	20	11	6	12	5	1.0	0.949	1.000
sp|P11449|VTU1_DROME	P11449	Vm26Aa	4	19	12	11	7	18	12	4	12	3	1.0	0.966	1.000
tr|Q9VJN0|Q9VJN0_DROME	Q9VJN0	CG31821	0	15	0	1	8	6	5	5	5	2	1.0	0.994	1.000
tr|Q9VHK7|Q9VHK7_DROME	Q9VHK7	CG8369	0	17	10	0	13	14	9	5	9	5	1.0	1.000	1.000

tr|Q8MT58|Q8MT58_DROME	Q8MT58	CG17337	1	15	30		3	12	30		15	8		15	8		1.0	0.995	1.000
tr|Q9VUC1|Q9VUC1_DROME	Q9VUC1	Hsc70Cb	4	7	12		6	4	12		7	2		7	2		1.0	0.942	1.000
sp|P48375|FKB12_DROME	P48375	FK506-bp2	12	13	26		8	19	22		17	4		16	4		0.9	0.894	1.000
tr|O97102|O97102_DROME	O97102	smt3	3	3	4		2	3	4		3	0		3	0		0.9	0.775	1.000
tr|Q7KRU8|Q7KRU8_DROME	Q7KRU8	Fer1HCH	28	156	214		26	108	236		133	55		123	61		0.9	0.917	1.000
sp|Q9V496|APLP_DROME	Q9V496	Rfabg	829	3533	2418		1111	2095	3086		2260	785		2097	570		0.9	0.875	1.000
tr|Q8INK2|Q8INK2_DROME	Q8INK2	fabp	11	11	16		11	5	18		13	2		12	4		0.9	0.797	1.000
tr|Q9V3U6|Q9V3U6_DROME	Q9V3U6	26-29-p	4	3	8		2	5	6		5	2		4	1		0.9	0.830	1.000
tr|Q9I7Q5|Q9I7Q5_DROME	Q9I7Q5	Cpr65Au	7	17	0		4	9	8		8	5		7	2		0.9	0.873	1.000
sp|Q9W303|IDGF4_DROME	Q9W303	Idgf4	31	185	54		54	96	88		90	48		79	13		0.9	0.839	1.000
tr|Q9VZR2|Q9VZR2_DROME	Q9VZR2	Drsl5	0	5	20		0	0	22		8	6		7	7		0.9	0.912	1.000

Group 4: In both w^{1118} and mutant but <0.8 lower in $dKlf15^{NN}$ mutant

	Uniprot ID	Annotation	w1118				dKlf15NN				w1118			dKlf15NN				
			#1	#2	#3		#1	#2	#3		Mean	SEM		Mean	SEM		Fold chang	t-Test	B-H Correction
sp|Q05825|ATPB_DROME	Q05825	ATPsyn-beta	62	15	46		6	0	0		41	14		2	2		0.1	0.051	0.164
sp|P05661-17|MYSA_DROME	P05661-17	Mhc	264	47	158		42	0	0		156	63		14	14		0.1	0.092	0.193
sp|P18432|MLR_DROME	P18432	Mlc2	39	12	8		8	0	0		20	10		3	3		0.1	0.167	0.295
tr|Q960M4|Q960M4_DROME	Q960M4	Prx5	19	20	8		5	3	0		16	4		2	1		0.2	0.033	0.130
tr|O76935|O76935_DROME	O76935	Irp-1B	12	33	22		6	5	0		22	6		4	2		0.2	0.043	0.156
sp|P08736|EF1A1_DROME	P08736	Ef1alpha48D	26	29	152		9	25	0		69	41		11	7		0.2	0.242	0.396
sp|P13060-1|EF2_DROME	P13060	Ef2b	32	23	44		5	7	6		33	6		6	1		0.2	0.012	0.091
tr|Q9W330|Q9W330_DROME	Q9W330	Hex-A	100	92	30		33	7	0		74	22		13	10		0.2	0.066	0.180
sp|Q9W401-1|CISY_DROME	Q9W401	kdn	81	44	84		18	13	8		70	13		13	3		0.2	0.013	0.091
sp|P31409|VATB_DROME	P31409	Vha55	13	5	18		5	3	0		12	4		2	1		0.2	0.072	0.180
tr|Q24349|Q24349_DROME	Q24349	Gdi	6	9	14		6	0	0		10	2		2	2		0.2	0.073	0.180
sp|P13706-2|GPDA_DROME	P13706-2	Gpdh	683	1108	776		268	309	0		856	129		192	97		0.2	0.015	0.091
sp|Q24560|TBB1_DROME	Q24560	betaTub56D	36	36	22		10	12	0		31	5		7	4		0.2	0.015	0.091
sp|Q9VWH4-1|IDH3A_DROME	Q9VWH4	l(1)G0156	25	16	38		7	5	6		26	6		6	1		0.2	0.034	0.130
sp|Q9Y0Y2|PURA_DROME	Q9Y0Y2	CG17273	19	12	16		7	4	0		16	2		4	2		0.2	0.014	0.091
tr|Q8IQW5|Q8IQW5_DROME	Q8IQW5	HspB8	13	23	14		6	3	4		16	3		4	1		0.2	0.019	0.109
sp|P20478-1|GLNA2_DROME	P20478	Gs2	34	29	28		10	9	4		30	2		8	2		0.3	0.001	0.034
sp|P06603|TBA1_DROME	P06603	alphaTub84B	30	25	62		13	17	0		39	12		10	5		0.3	0.084	0.193
sp|P92177-1|1433E_DROME	P92177-1	14-3-3epsilon	10	27	28		0	11	6		21	6		6	3		0.3	0.075	0.180
tr|Q9VLS4|Q9VLS4_DROME	Q9VLS4	CG8498	15	9	0		6	0	0		8	4		2	2		0.3	0.287	0.428
tr|Q9VQB4|Q9VQB4_DROME	Q9VQB4	CG3609	8	16	6		0	4	4		10	3		3	1		0.3	0.089	0.193
tr|Q8IPA2|Q8IPA2_DROME	Q8IPA2	Mal-B2	6	27	2		0	9	0		12	8		3	3		0.3	0.365	0.482
sp|P42281|ACBP_DROME	P42281	Dbi	0	15	28		0	12	0		14	8		4	4		0.3	0.320	0.458
tr|B7Z001|B7Z001_DROME	B7Z001	CG3523	91	208	174		39	47	48		158	35		45	3		0.3	0.032	0.130
tr|Q9VU38|Q9VU38_DROME	Q9VU38	AdenoK	6	13	8		2	5	0		9	2		3	2		0.3	0.072	0.180
sp|P41043|GST1_DROME	P41043	GstS1	60	60	64		27	20	6		61	1		18	6		0.3	0.002	0.039
sp|P84029|CYC2_DROME	P84029	Cyt-c-p	12	67	12		2	20	4		30	18		9	6		0.3	0.325	0.459
tr|A8DZ21|A8DZ21_DROME	A8DZ21	Acon	72	31	96		18	15	26		66	19		20	3		0.3	0.074	0.180
sp|Q7KN62-1|TERA_DROME	Q7KN62	TER94	10	7	16		7	3	0		11	3		3	2		0.3	0.087	0.193
tr|Q9VKI8|Q9VKI8_DROME	Q9VKI8	CG6287	15	23	26		6	7	6		21	3		6	0		0.3	0.011	0.091
sp|P29310-2|1433Z_DROME	P29310-2	14-3-3zeta	0	107	78		0	20	36		62	32		19	10		0.3	0.270	0.414
sp|P52034-1|K6PF_DROME	P52034	Pfk	111	80	68		50	27	4		86	13		27	13		0.3	0.033	0.130
sp|P11147|HSP7D_DROME	P11147	Hsc70-4	20	49	86		17	15	18		52	19		16	1		0.3	0.138	0.258
tr|Q8IQ18|Q8IQ18_DROME	Q8IQ18	Dp	14	23	0		12	0	0		12	7		4	4		0.3	0.344	0.472
sp|P07764-1|ALF_DROME	P07764	Ald	728	1353	674		292	281	332		919	218		302	15		0.3	0.048	0.159
sp|P52029|G6PI_DROME	P52029	Pgi	119	212	122		50	48	52		151	30		50	1		0.3	0.030	0.130
sp|Q9VUY9|PGM_DROME	Q9VUY9	Pgm	27	69	38		16	21	8		45	13		15	4		0.3	0.090	0.193
sp|Q9VFC8-1|GYS_DROME	Q9VFC8	CG6904	74	64	66		24	28	20		68	3		24	2		0.4	0.000	0.000
tr|Q8IQF8|Q8IQF8_DROME	Q8IQF8	CG6084	12	24	34		8	17	0		23	6		8	5		0.4	0.141	0.259
sp|P29310-1|1433Z_DROME	P29310	14-3-3zeta	94	109	86		42	27	36		96	7		35	5		0.4	0.002	0.039
tr|Q9Y119|Q9Y119_DROME	Q9Y119	Tps1	34	51	68		22	31	4		51	10		19	8		0.4	0.063	0.180
tr|Q9VEB1|Q9VEB1_DROME	Q9VEB1	Mdh2	44	37	64		17	12	26		48	8		18	4		0.4	0.028	0.130
sp|P91938-1|TRXR1_DROME	P91938	Trxr-1	8	25	26		3	12	8		20	6		8	3		0.4	0.129	0.246
tr|Q9Y112|Q9Y112_DROME	Q9Y112	BcDNA.GH10614	4	12	26		2	11	4		14	6		5	3		0.4	0.295	0.434
tr|E1JGQ5|E1JGQ5_DROME	E1JGQ5	CG9485	0	76	0		10	9	10		25	25		10	0		0.4	0.576	0.674
sp|P83967|ACT6_DROME	P83967	Act88F	117	93	128		67	65	0		113	10		44	22		0.4	0.048	0.159
sp|P48602|VATA1_DROME	P48602	Vha68-1	10	15	0		7	3	0		8	4		3	2		0.4	0.353	0.472
sp|Q9XTL9|PYG_DROME	Q9XTL9	GlyP	423	597	520		184	221	202		513	50		202	11		0.4	0.004	0.046
sp|P29613-1|TPIS_DROME	P29613-1	Tpi	172	233	202		90	76	78		203	18		81	4		0.4	0.003	0.039
sp|O62619-1|KPYK_DROME	O62619	PyK	375	492	382		170	161	172		416	38		168	3		0.4	0.003	0.039
tr|Q8IQG9|Q8IQG9_DROME	Q8IQG9	Adk1	14	23	18		9	9	4		18	2		7	2		0.4	0.022	0.119
tr|Q9VGB6|Q9VGB6_DROME	Q9VGB6	Pglym87	20	20	38		10	8	14		26	6		11	2		0.4	0.070	0.180
sp|Q01604|PGK_DROME	Q01604	Pgk	245	244	280		125	93	102		256	12		107	9		0.4	0.001	0.034
tr|A1Z7Z4|A1Z7Z4_DROME	A1Z7Z4	CG1648	3	4	12		0	8	0		6	3		3	3		0.4	0.401	0.511
tr|Q7KSU6|Q7KSU6_DROME	Q7KSU6	CG8036	12	20	72		15	11	18		35	19		15	2		0.4	0.350	0.472
tr|Q961N7|Q961N7_DROME	Q961N7	CG5355	9	12	4		4	3	4		8	2		4	0		0.4	0.115	0.230
sp|P17336|CATA_DROME	P17336	Cat	10	45	42		8	20	14		32	11		14	3		0.4	0.197	0.338
tr|Q9VK60|Q9VK60_DROME	Q9VK60	CG6180	10	24	24		10	8	8		19	5		9	1		0.4	0.089	0.193
sp|Q9I7S8|PUR6_DROME	Q9I7S8	ade5	7	23	10		3	15	0		13	5		6	4		0.4	0.316	0.458
sp|P15007-1|ENO_DROME	P15007	Eno	760	1099	624		402	359	346		827	141		369	17		0.4	0.032	0.130
sp|P07486|G3P1_DROME	P07486	Gapdh1	785	935	592		391	300	348		771	99		346	26		0.4	0.014	0.091
sp|P02828|HSP83_DROME	P02828	Hsp83	31	43	74		21	24	26		49	13		24	2		0.5	0.116	0.230
tr|Q9VF24|Q9VF24_DROME	Q9VF24	cv-d	3	56	14		10	13	12		24	16		12	1		0.5	0.477	0.591
tr|Q95RT1|Q95RT1_DROME	Q95RT1	CG11089	5	12	10		4	9	0		9	2		4	3		0.5	0.241	0.396
sp|P48610-1|KARG_DROME	P48610	Argk	465	588	532		246	243	296		528	36		261	17		0.5	0.003	0.039
sp|P07487|G3P2_DROME	P07487	Gapdh2	724	864	598		404	356	334		729	77		365	21		0.5	0.010	0.091
tr|B7Z0E0|B7Z0E0_DROME	B7Z0E0	Idh	22	27	28		13	20	6		26	2		13	4		0.5	0.044	0.156
tr|Q8MSI2|Q8MSI2_DROME	Q8MSI2	Scp1	27	235	426		14	124	208		229	115		115	56		0.5	0.425	0.534
sp|P45594|CADF_DROME	P45594	tsr	22	24	22		7	11	18		23	1		12	3		0.5	0.032	0.130
sp|P00334|ADH_DROME	P00334	Adh	303	572	472		201	251	266		449	79		239	20		0.5	0.061	0.180
sp|P02572|ACT2_DROME	P02572	Act42A	64	67	126		0	60	78		86	20		46	24		0.5	0.271	0.414
sp|P08879|NDKA_DROME	P08879	awd	0	53	126		1	15	84		60	37		33	26		0.6	0.583	0.675
sp|Q9VGS2|TCTP_DROME	Q9VGS2	Tctp	8	11	12		3	8	6		10	1		6	1		0.6	0.063	0.180
tr|Q8MQS7|Q8MQS7_DROME	Q8MQS7	Mdh1	28	48	24		18	33	4		33	7		19	8		0.6	0.265	0.414
sp|Q9V3P0|PRDX1_DROME	Q9V3P0	Jafrac1	21	40	30		10	21	20		30	6		17	3		0.6	0.115	0.230
sp|Q9VAN0|SERC_DROME	Q9VAN0	CG11899	4	11	8		3	4	6		8	2		4	1		0.6	0.169	0.295
tr|Q7KT11|Q7KT11_DROME	Q7KT11	CG9331	5	15	32		10	12	8		17	8		10	1		0.6	0.402	0.511
sp|Q9VZ49|ENDOU_DROME	Q9VZ49	CG2145	1	17	0		8	3	0		6	6		4	2		0.6	0.707	0.751
tr|Q9VM18|Q9VM18_DROME	Q9VM18	CG5177	13	11	22		7	12	8		15	3		9	1		0.6	0.166	0.295
tr|Q24450|Q24450_DROME	Q24450	Pglym78	18	19	36		12	9	22		24	6		14	4		0.6	0.239	0.396
sp|O77460|IPYR_DROME	O77460	Nurf-38	24	44	46		20	29	20		38	7		23	3		0.6	0.127	0.246
tr|Q9U1I4|Q9U1I4_DROME	Q9U1I4	Spn88Ea	0	27	18		2	0	26		15	8		9	8		0.6	0.647	0.717
sp|Q8IR95|Q8IR95_DROME	Q8IR95	CG32667	0	23	8		0	9	10		10	7		6	3		0.6	0.636	0.715
tr|Q7JVX3|Q7JVX3_DROME	Q7JVX3	CG4408	7	49	24		11	11	30		27	12		17	6		0.6	0.521	0.617
sp|P46415|ADHX_DROME	P46415	Fdh	7	4	20		6	11	4		10	5		7	2		0.6	0.517	0.617
tr|Q7KT33|Q7KT33_DROME	Q7KT33	fbp	9	17	12		6	13	6		13	2		8	3		0.7	0.273	0.414
sp|Q24388|LSP2_DROME	Q24388	Lsp2	22	65	20		0	3	68		36	15		24	22		0.7	0.674	0.737

sp|P61851|SODC_DROME	P61851	Sod	35	45	76		20	31	54		52	12		35	10		0.7	0.338	0.470
sp|P20432|GSTT1_DROME	P20432	GstD1	13	31	56		10	19	38		33	13		22	8		0.7	0.513	0.617
tr|Q9VGA0|Q9VGA0_DROME	Q9VGA0	GstD9	12	11	0		6	8	2		8	4		5	2		0.7	0.605	0.692
sp|P25007|PPIA_DROME	P25007	Cyp1	26	37	54		19	28	34		39	8		27	4		0.7	0.258	0.414
sp|P0CG69|UBIQP_DROME	P0CG69	Ubi-p63E	3	4	24		2	4	16		10	7		7	4		0.7	0.741	0.763
sp|Q9V429-1|THIO2_DROME	Q9V429	Trx-2	6	5	6		3	5	4		6	0		4	1		0.7	0.073	0.180
tr|Q9VHA1|Q9VHA1_DROME	Q9VHA1	SpdS	3	7	0		2	3	2		3	2		2	0		0.7	0.680	0.737
sp|P36951|HYI_DROME	P36951	Gip	4	17	6		3	11	6		9	4		7	2		0.7	0.639	0.715
sp|P02574|ACT4_DROME	P02574	Act79B	89	77	0		55	68	0		55	28		41	21		0.7	0.702	0.751
sp|Q02748|IF4A_DROME	Q02748	eIF-4a	14	17	18		5	11	22		17	1		12	5		0.8	0.482	0.591
tr|Q9W370|Q9W370_DROME	Q9W370	CG15369	14	21	12		14	7	16		16	3		12	3		0.8	0.399	0.511
tr|Q9U4U2|Q9U4U2_DROME	Q9U4U2	Fer2LCH	25	231	270		29	136	250		175	76		138	64		0.8	0.730	0.763
sp|P05303|EF1A2_DROME	P05303	Ef1alpha100E	34	27	0		10	23	16		20	10		16	4		0.8	0.736	0.763
tr|Q8SXA6|Q8SXA6_DROME	Q8SXA6	CG6045	7	36	6		9	19	12		16	10		13	3		0.8	0.780	0.795
tr|Q961T9|Q961T9_DROME	Q961T9	BG:DS00941.11	0	11	0		0	3	6		4	4		3	2		0.8	0.874	0.874
tr|Q8SXB9|Q8SXB9_DROME	Q8SXB9	CG10433	4	28	18		5	9	28		17	7		14	7		0.8	0.813	0.821

Group 5:

Present in w^{1118} control but undetected in $dKlf15^{NN}$ mutant
(a mean of two spectral counts or lower was regarded as undetected)

	Uniprot ID	Annotation	w1118				dKlf15NN				w1118			dKlf15NN				
			#1	#2	#3		#1	#2	#3		Mean	SEM		Mean	SEM		t-Test	B-H Correction
tr|E1JI91|E1JI91_DROME	E1JI91	UGP	90	105	0		0	0	0		65	33		0	0		0.118	0.407
sp|P53501|ACT3_DROME	P53501	Act57B	0	0	106		0	0	0		35	35		0	0		0.374	0.407
tr|Q7KVP4|Q7KVP4_DROME	Q7KVP4	CG9485	48	0	44		0	0	0		31	15		0	0		0.117	0.407
tr|A1ZA66|A1ZA66_DROME	A1ZA66	Strn-Mlck	45	0	28		0	0	0		24	13		0	0		0.137	0.407
sp|P35381|ATPA_DROME	P35381	blw	37	9	16		5	0	0		21	8		2	2		0.085	0.407
sp|P19889|RLA0_DROME	P19889	RpLP0	11	3	32		0	0	0		15	9		0	0		0.154	0.407
tr|A1Z992|A1Z992_DROME	A1Z992	AGBE	6	29	10		0	0	0		15	7		0	0		0.104	0.407
tr|A8JNU6|A8JNU6_DROME	A8JNU6	Nc73EF	34	9	0		0	0	0		15	10		0	0		0.229	0.407
sp|P08570|RLA1_DROME	P08570	RpLP1	7	7	26		2	0	0		13	6		1	1		0.130	0.407
sp|Q27331|VATA2_DROME	Q27331	Vha68-2	13	11	16		0	0	0		13	2		0	0		0.001	0.075
tr|A8JRB8|A8JRB8_DROME	A8JRB8	CG5028-RC	13	9	16		4	0	0		13	2		1	1		0.008	0.224
sp|P11996|LSP1B_DROME	P11996	Lsp1beta	10	28	0		2	0	0		13	8		1	1		0.227	0.407
sp|O96827|EF1B_DROME	O96827	Ef1beta	6	4	26		3	0	0		12	7		1	1		0.199	0.407
tr|Q9VGQ1|Q9VGQ1_DROME	Q9VGQ1	CG5214	15	8	12		0	0	0		12	2		0	0		0.004	0.149
tr|Q8T447|Q8T447_DROME	Q8T447	CG9961	0	0	34		0	0	0		11	11		0	0		0.374	0.407
tr|E2QCF1|E2QCF1_DROME	E2QCF1	ATPCL	4	16	12		3	0	0		11	3		1	1		0.051	0.407
tr|Q9VJZ6|Q9VJZ6_DROME	Q9VJZ6	CG6523	10	15	8		6	0	0		11	2		2	2		0.031	0.407
sp|P05389|RLA2_DROME	P05389	RpLP2	4	5	22		2	0	0		11	6		1	1		0.154	0.407
sp|P55830-1|RS3A_DROME	P55830	RpS3A	4	5	20		0	0	0		10	5		0	0		0.120	0.407
tr|B7Z0V3|B7Z0V3_DROME	B7Z0V3	CG2767	5	16	8		2	0	0		10	3		1	1		0.055	0.407
sp|Q06559|RS3_DROME	Q06559	RpS3	5	0	24		0	0	0		10	7		0	0		0.252	0.407
tr|C0PUZ9|C0PUZ9_DROME	C0PUZ9	Glycogenin-RB	0	17	10		0	0	0		9	5		0	0		0.144	0.407
tr|Q95U38|Q95U38_DROME	Q95U38	skap	15	4	8		0	0	0		9	3		0	0		0.048	0.407
sp|Q9VU68-1|WDR1_DROME	Q9VU68	flr	10	7	10		2	0	0		9	1		1	1		0.004	0.149
tr|Q8MST5|Q8MST5_DROME	Q8MST5	betaTub97EF	13	13	0		0	0	0		9	4		0	0		0.116	0.407
tr|O16043|O16043_DROME	O16043	Df31	0	0	26		0	0	0		9	9		0	0		0.374	0.407
tr|Q5U0Z2|Q5U0Z2_DROME	Q5U0Z2	CG10576	0	0	26		0	0	0		9	9		0	0		0.374	0.407
sp|P53777|MLP1_DROME	P53777	Mlp60A	10	3	12		2	0	0		8	3		1	1		0.065	0.407
tr|Q9VSU6|Q9VSU6_DROME	Q9VSU6	Dhpr	7	17	0		5	0	0		8	5		2	2		0.275	0.407
sp|P38979-1|RSSA_DROME	P38979	sta	5	1	18		0	0	0		8	5		0	0		0.179	0.407
sp|P25843|PROF_DROME	P25843	chic	11	13	0		2	1	0		8	4		1	1		0.174	0.407
sp|Q8MLY8|RS8_DROME	Q8MLY8	RpS8	6	4	14		0	0	0		8	3		0	0		0.059	0.407
tr|Q9VI04|Q9VI04_DROME	Q9VI04	pyd3	9	15	0		2	0	0		8	4		1	1		0.179	0.407
tr|Q7K860|Q7K860_DROME	Q7K860	TpnC4	7	7	10		6	0	0		8	1		2	2		0.052	0.407
tr|Q8MLU2|Q8MLU2_DROME	Q8MLU2	CG11474	7	9	6		2	0	0		8	1		1	1		0.003	0.149
sp|Q9VNA5|PSB4_DROME	Q9VNA5	Prosbeta7	3	9	10		0	0	0		7	2		0	0		0.029	0.407
sp|Q9NJH0|EF1G_DROME	Q9NJH0	Ef1gamma	2	4	16		3	0	0		7	4		1	1		0.227	0.407
sp|P02825|HSP71_DROME	P02825	Hsp70Ab	0	0	22		0	0	0		7	7		0	0		0.374	0.407
sp|P14318|MP20_DROME	P14318	Mp20	5	3	14		0	0	0		7	3		0	0		0.101	0.407
tr|Q7JYW9|Q7JYW9_DROME	Q7JYW9	Hex-C	4	17	0		2	1	0		7	5		1	1		0.314	0.407
tr|O46111|O46111_DROME	O46111	Uba1	13	8	0		6	0	0		7	4		2	2		0.289	0.407
tr|Q9VPZ5|Q9VPZ5_DROME	Q9VPZ5	CG5397	0	21	0		4	0	0		7	7		1	1		0.469	0.491
sp|P14130|RS14_DROME	P14130	RpS14a	4	0	16		3	0	0		7	5		1	1		0.304	0.407
sp|P55828|RS20_DROME	P55828	RpS20	0	0	20		0	0	0		7	7		0	0		0.374	0.407
tr|Q8MS44|Q8MS44_DROME	Q8MS44	CG9468	0	0	20		0	0	0		7	7		0	0		0.374	0.407
tr|Q0KIE6|Q0KIE6_DROME	Q0KIE6	CG12582	0	20	0		3	0	0		7	7		1	1		0.453	0.481
sp|O16797-1|RL3_DROME	O16797	RpL3	5	3	12		3	0	0		7	3		1	1		0.135	0.407
tr|Q9XYZ9|Q9XYZ9_DROME	Q9XYZ9	GstE12	5	3	12		4	0	0		7	3		1	1		0.161	0.407
sp|Q94529|GS1_DROME	Q94529	Gs1l	5	15	0		0	0	0		7	4		0	0		0.197	0.407
tr|Q9W1B9|Q9W1B9_DROME	Q9W1B9	RpL12	4	0	16		0	0	0		7	5		0	0		0.245	0.407
sp|P22769|PSA71_DROME	P22769	Pros28.1	3	11	6		0	0	0		7	2		0	0		0.043	0.407
tr|Q8MT28|Q8MT28_DROME	Q8MT28	CG10467	0	13	6		0	0	0		6	4		0	0		0.170	0.407
sp|P12881|PSA1_DROME	P12881	Pros35	5	8	6		0	0	0		6	1		0	0		0.001	0.075
sp|P46222|RL11_DROME	P46222	RpL11	3	4	12		0	0	0		6	3		0	0		0.091	0.407
sp|Q6AWN0|MTND_DROME	Q6AWN0	CG32068	3	4	12		2	0	0		6	3		1	1		0.116	0.407
sp|P35554|FTN_DROME	P35554	fln	7	0	12		0	0	0		6	3		0	0		0.147	0.407
tr|Q76NQ9|Q76NQ9_DROME	Q76NQ9	AMPdeam	8	4	6		2	0	0		6	1		1	1		0.022	0.407
tr|Q7K3J0|Q7K3J0_DROME	Q7K3J0	CG8258	7	3	8		0	0	0		6	2		0	0		0.023	0.407
tr|Q9VQF7|Q9VQF7_DROME	Q9VQF7	Bacc	0	4	14		0	3	0		6	4		1	1		0.296	0.407
tr|Q6WSQ9|Q6WSQ9_DROME	Q6WSQ9	Mitf	0	0	18		0	0	0		6	6		0	0		0.374	0.407
tr|Q95SI7|Q95SI7_DROME	Q95SI7	CG6028	6	8	4		1	0	0		6	1		0	0		0.008	0.224
sp|P18091-1|ACTN_DROME	P18091	Actn	18	0	0		0	0	0		6	6		0	0		0.374	0.407
tr|Q9VA37|Q9VA37_DROME	Q9VA37	dj-1beta	3	11	4		0	0	2		6	2		1	1		0.105	0.407
sp|P41042|RS4_DROME	P41042	RpS4	1	0	16		0	0	0		6	5		0	0		0.317	0.407
tr|Q8MYS9|Q8MYS9_DROME	Q8MYS9	CG7203	7	11	0		2	0	0		6	3		1	1		0.195	0.407
sp|P35122|UCHL_DROME	P35122	Uch	0	9	8		0	0	0		6	3		0	0		0.118	0.407
sp|P32100|RL7_DROME	P32100	RpL7	3	0	14		0	0	0		6	4		0	0		0.254	0.407
sp|P48159|RL23_DROME	P48159	RpL23	3	0	14		0	0	0		6	4		0	0		0.254	0.407
tr|Q9VV75|Q9VV75_DROME	Q9VV75	CG4169	9	0	8		0	0	0		6	3		0	0		0.117	0.407
tr|Q8IRQ5|Q8IRQ5_DROME	Q8IRQ5	l(1)G0255	7	9	0		0	0	0		6	3		0	0		0.121	0.407
tr|Q9W3L4|Q9W3L4_DROME	Q9W3L4	CG2233	0	11	6		0	0	0		6	3		0	0		0.146	0.407
tr|Q9VD58|Q9VD58_DROME	Q9VD58	CG6439	10	0	6		0	0	0		5	3		0	0		0.144	0.407
tr|Q7K5K3|Q7K5K3_DROME	Q7K5K3	CG11876	9	1	6		0	0	0		5	2		0	0		0.071	0.407
sp|Q94518|NACA_DROME	Q94518	Nacalpha	2	0	14		2	0	0		5	4		1	1		0.327	0.407
sp|P09180|RL4_DROME	P09180	RpL4	8	0	8		0	0	0		5	3		0	0		0.116	0.407
tr|Q9VTZ0|Q9VTZ0_DROME	Q9VTZ0	tral	0	0	16		0	0	0		5	5		0	0		0.374	0.407
sp|P29327-1|RS6_DROME	P29327	RpS6	6	0	10		0	0	0		5	3		0	0		0.141	0.407
tr|Q9GQV2|Q9GQV2_DROME	Q9GQV2	cher	16	0	0		0	0	0		5	5		0	0		0.374	0.407
tr|Q9VN21|Q9VN21_DROME	Q9VN21	lost	1	0	14		0	0	0		5	4		0	0		0.309	0.407
sp|O18640|GBLP_DROME	O18640	Rack1	0	1	14		0	0	0		5	4		0	0		0.316	0.407
tr|Q9VW19|Q9VW19_DROME	Q9VW19	CG9372	0	13	2		0	4	0		5	4		1	1		0.435	0.466
sp|A1ZA47-1|ZASP_DROME	A1ZA47	Zasp52	6	5	4		0	0	0		5	1		0	0		0.001	0.075

sp|P06742-1|MLC1_DROME	P06742	Mlc1	11	0	4		0	0	0		5	3		0	0		0.197	0.407
tr|Q9VB64|Q9VB64_DROME	Q9VB64	CG31063	0	7	8		0	1	4		5	2		2	1		0.320	0.407
tr|Q961R8|Q961R8_DROME	Q961R8	Aats-gly	5	9	0		0	0	0		5	3		0	0		0.147	0.407
tr|Q9I7R0|Q9I7R0_DROME	Q9I7R0	CG18815	2	4	8		0	0	0		5	2		0	0		0.050	0.407
sp|Q26365-2|ADT_DROME	Q26365-2	sesB	14	0	0		0	0	0		5	5		0	0		0.374	0.407
sp|P29844|HSP7C_DROME	P29844	Hsc70-3	0	0	14		0	0	0		5	5		0	0		0.374	0.407
sp|P50882|RL9_DROME	P50882	RpL9	0	0	14		0	0	0		5	5		0	0		0.374	0.407
tr|Q86BQ4|Q86BQ4_DROME	Q86BQ4	CG2862	6	8	0		4	0	0		5	2		1	1		0.293	0.407
sp|Q9W0P5|GALE_DROME	Q9W0P5	Gale	4	9	0		0	0	0		5	3		0	0		0.163	0.407
tr|A8JUT4|A8JUT4_DROME	A8JUT4	Ntf-2	4	9	0		0	0	0		5	3		0	0		0.163	0.407
sp|P49630|RL36_DROME	P49630	RpL36	1	0	12		0	0	0		4	4		0	0		0.299	0.407
tr|Q7JX87|Q7JX87_DROME	Q7JX87	Prx2540-2	1	12	0		4	0	0		4	4		1	1		0.474	0.494
tr|Q7KTK9|Q7KTK9_DROME	Q7KTK9	CG5261	13	0	0		0	0	0		4	4		0	0		0.374	0.407
sp|Q27415-1|NLP_DROME	Q27415	Nlp	2	0	10		0	0	0		4	3		0	0		0.249	0.407
sp|P48149|RS15A_DROME	P48149	RpS15Aa	2	0	10		3	0	0		4	3		1	1		0.401	0.434
sp|P06754-1|TPM1_DROME	P06754-1	Tm1	1	3	8		0	0	0		4	2		0	0		0.113	0.407
sp|Q9W5R8|RL5_DROME	Q9W5R8	RpL5	0	0	12		0	0	0		4	4		0	0		0.374	0.407
tr|Q8MT23|Q8MT23_DROME	Q8MT23	RpL30	0	0	12		0	0	0		4	4		0	0		0.374	0.407
tr|Q8INP8|Q8INP8_DROME	Q8INP8	CG11980	5	7	0		0	0	0		4	2		0	0		0.122	0.407
sp|Q27580|SAHH_DROME	Q27580	Ahcy13	4	8	0		0	0	0		4	2		0	0		0.166	0.407
tr|Q9VXQ5|Q9VXQ5_DROME	Q9VXQ5	Tcp-1zeta	4	0	8		0	0	0		4	2		0	0		0.166	0.407
sp|Q9GU68|IF5A_DROME	Q9GU68	eIF-5A	4	0	8		5	0	0		4	2		2	2		0.457	0.483
sp|P55841|RL14_DROME	P55841	RpL14	1	0	10		0	0	0		4	3		0	0		0.286	0.407
sp|P20241-1|NRG_DROME	P20241	Nrg	1	7	4		0	1	0		4	2		0	0		0.130	0.407
tr|Q9VSL2|Q9VSL2_DROME	Q9VSL2	GstO3	0	5	6		0	0	0		4	2		0	0		0.117	0.407
sp|Q9VA91|RS7_DROME	Q9VA91	RpS7	3	0	8		0	0	0		4	2		0	0		0.192	0.407
sp|Q9V9X4|MTNA_DROME	Q9V9X4	CG11334	1	1	8		0	0	0		4	2		0	0		0.176	0.407
sp|Q8IRH0|Q8IRH0_DROME	Q8IRH0	Psa	7	4	0		3	0	0		4	2		1	1		0.323	0.407
tr|Q9W2M4|Q9W2M4_DROME	Q9W2M4	CG10527	0	7	4		0	3	0		4	2		1	1		0.279	0.407
sp|Q9VMR8|TOTM_DROME	Q9VMR8	TotM	0	11	0		0	1	0		4	4		0	0		0.434	0.466
tr|Q8SXV8|Q8SXV8_DROME	Q8SXV8	CG3246	0	11	0		0	5	0		4	4		2	2		0.678	0.690
sp|P29843|HSP7A_DROME	P29843	Hsc70-1	5	5	0		0	0	0		4	2		0	0		0.116	0.407
sp|Q94522|SUCA_DROME	Q94522	Scsalpha	2	0	8		1	0	0		3	2		0	0		0.260	0.407
sp|P02518|HSP27_DROME	P02518	Hsp27	0	0	10		0	0	0		3	3		0	0		0.374	0.407
sp|P55935|RS9_DROME	P55935	RpS9	0	0	10		0	0	0		3	3		0	0		0.374	0.407
tr|Q0E9I6|Q0E9I6_DROME	Q0E9I6	Dscam1	0	0	10		0	0	0		3	3		0	0		0.374	0.407
tr|Q7JW48|Q7JW48_DROME	Q7JW48	CG10911	0	0	10		0	0	0		3	3		0	0		0.374	0.407
tr|Q9VBR8|Q9VBR8_DROME	Q9VBR8	CG11902	0	0	10		0	0	0		3	3		0	0		0.374	0.407
sp|P22464-1|ANXB9_DROME	P22464	AnnIX	4	1	4		0	0	0		3	1		0	0		0.029	0.407
sp|P09491-1|TPM2_DROME	P09491	Tm2	4	5	0		0	0	0		3	2		0	0		0.119	0.407
tr|Q9VPX6|Q9VPX6_DROME	Q9VPX6	capt	4	5	0		0	0	0		3	2		0	0		0.119	0.407
sp|Q24407|ATP5J_DROME	Q24407	ATPsyn-Cf6	4	0	6		0	0	0		3	2		0	0		0.137	0.407
tr|Q7KVX1|Q7KVX1_DROME	Q7KVX1	l(1)G0334	7	0	2		0	0	0		3	2		0	0		0.230	0.407
tr|Q9V3W0|Q9V3W0_DROME	Q9V3W0	UK114	0	1	8		0	0	0		3	2		0	0		0.277	0.407
sp|Q00174|LAMA_DROME	Q00174	LanA	0	9	0		0	0	0		3	3		0	0		0.374	0.407
tr|Q9VNK6|Q9VNK6_DROME	Q9VNK6	CG11459	0	9	0		0	0	0		3	3		0	0		0.374	0.407
tr|O96299|O96299_DROME	O96299	Sodh-2	2	7	0		0	0	0		3	2		0	0		0.204	0.407
tr|Q9VM19|Q9VM19_DROME	Q9VM19	CG5171	2	7	0		1	0	0		3	2		0	0		0.243	0.407
sp|P54385-1|DHE3_DROME	P54385	Gdh	4	0	4		0	0	0		3	1		0	0		0.117	0.407
sp|P17704|RS17_DROME	P17704	RpS17	2	0	6		0	0	0		3	2		0	0		0.192	0.407
sp|P41044|CAB32_DROME	P41044	Cbp53E	8	0	0		0	0	0		3	3		0	0		0.374	0.407
sp|O61231|RL10_DROME	O61231	RpL10	0	0	8		0	0	0		3	3		0	0		0.374	0.407
sp|O76454|PHS_DROME	O76454	Pcd	0	0	8		0	0	0		3	3		0	0		0.374	0.407
sp|P02517|HSP26_DROME	P02517	Hsp26	0	0	8		0	0	0		3	3		0	0		0.374	0.407
sp|P23128-1|DDX6_DROME	P23128	me31B	0	0	8		0	0	0		3	3		0	0		0.374	0.407
sp|P49847|TAF6_DROME	P49847	Taf6	0	0	8		0	0	0		3	3		0	0		0.374	0.407
sp|Q9V3S0|CP4G1_DROME	Q9V3S0	Cyp4g1	0	0	8		0	0	0		3	3		0	0		0.374	0.407
sp|Q9V597|RL31_DROME	Q9V597	RpL31	0	0	8		0	0	0		3	3		0	0		0.374	0.407
tr|A1Z892|A1Z892_DROME	A1Z892	Prx2540-1	0	0	8		0	0	0		3	3		0	0		0.374	0.407
tr|Q24150|Q24150_DROME	Q24150	Nap1	0	0	8		0	0	0		3	3		0	0		0.374	0.407
tr|Q9VTM9|Q9VTM9_DROME	Q9VTM9	CG32088	0	0	8		0	0	0		3	3		0	0		0.374	0.407
tr|A1ZAA5|A1ZAA5_DROME	A1ZAA5	Got1	5	3	0		0	0	0		3	2		0	0		0.156	0.407
sp|Q00637|SODM_DROME	Q00637	Sod2	4	0	4		0	0	0		3	1		0	0		0.117	0.407
tr|A1Z6X6|A1Z6X6_DROME	A1Z6X6	CG1707	2	5	0		0	0	0		3	2		0	0		0.178	0.407
sp|Q8T3U2|RS23_DROME	Q8T3U2	RpS23	1	0	6		0	0	0		2	2		0	0		0.238	0.407
sp|O02649|CH60_DROME	O02649	Hsp60	1	0	6		0	3	0		2	2		1	1		0.468	0.491
tr|Q9VJ31|Q9VJ31_DROME	Q9VJ31	CG10623	4	3	0		0	0	0		2	1		0	0		0.141	0.407
tr|Q9W3B3|Q9W3B3_DROME	Q9W3B3	CG1885	3	4	0		1	0	0		2	1		0	0		0.169	0.407
sp|Q9VLM8|SYAC_DROME	Q9VLM8	Aats-ala	7	0	0		0	0	0		2	2		0	0		0.374	0.407
sp|P15278-1|FAS3_DROME	P15278	Fas3	0	7	0		0	0	0		2	2		0	0		0.374	0.407
tr|A4V464|A4V464_DROME	A4V464	Acon	0	3	4		0	0	0		2	1		0	0		0.132	0.407
tr|Q8ST39|Q8ST39_DROME	Q8ST39	CG9336	0	3	4		0	1	0		2	1		0	0		0.230	0.407
tr|Q7KV27|Q7KV27_DROME	Q7KV27	CG1640	4	3	0		0	0	0		2	1		0	0		0.127	0.407
tr|Q8IP97|Q8IP97_DROME	Q8IP97	Pex19	4	3	0		2	0	0		2	1		1	1		0.264	0.407
tr|O76902|O76902_DROME	O76902	rush	2	0	4		0	0	0		2	1		0	0		0.147	0.407
tr|Q8SYA6|Q8SYA6_DROME	Q8SYA6	CG7322	2	4	0		1	0	0		2	1		0	0		0.202	0.407
sp|O18405|SURF4_DROME	O18405	Surf4	0	0	6		0	0	0		2	2		0	0		0.374	0.407
sp|P29742|CLH_DROME	P29742	Chc	0	0	6		0	0	0		2	2		0	0		0.374	0.407
sp|P46150-1|MOEH_DROME	P46150	Moe	0	0	6		0	0	0		2	2		0	0		0.374	0.407
sp|P46223|RL7A_DROME	P46223	RpL7A	0	0	6		0	0	0		2	2		0	0		0.374	0.407
sp|P48598-1|IF4E_DROME	P48598	eIF-4E	0	0	6		0	0	0		2	2		0	0		0.374	0.407
sp|P62152|CALM_DROME	P62152	Cam	0	0	6		0	0	0		2	2		0	0		0.374	0.407
sp|Q9VG97|GSTT3_DROME	Q9VG97	GstD3	0	0	6		0	0	0		2	2		0	0		0.374	0.407
sp|Q9VWG3|RS10B_DROME	Q9VWG3	RpS10b	0	0	6		0	0	0		2	2		0	0		0.374	0.407
tr|A8DZ02|A8DZ02_DROME	A8DZ02	kuz	0	0	6		0	0	0		2	2		0	0		0.374	0.407
tr|Q8MR43|Q8MR43_DROME	Q8MR43	CG1622	0	0	6		0	0	0		2	2		0	0		0.374	0.407
tr|Q9V9W2|Q9V9W2_DROME	Q9V9W2	RpL6	0	0	6		0	0	0		2	2		0	0		0.374	0.407
sp|Q26365-1|ADT_DROME	Q26365	sesB	0	0	6		2	0	0		2	2		1	1		0.607	0.621
sp|A1ZA47-4|ZASP_DROME	A1ZA47-4	Zasp52	6	0	0		0	0	0		2	2		0	0		0.374	0.407
tr|D1YSG0|D1YSG0_DROME	D1YSG0	bt	6	0	0		0	0	0		2	2		0	0		0.374	0.407
tr|Q8IPC2|Q8IPC2_DROME	Q8IPC2	CG13138	6	0	0		0	0	0		2	2		0	0		0.374	0.407
tr|Q9W2X6|Q9W2X6_DROME	Q9W2X6	l(1)G0230	6	0	0		1	0	0		2	2		0	0		0.439	0.468
sp|O01666|ATPG_DROME	O01666	ATPsyn-gamma	4	0	2		1	0	0		2	1		0	0		0.213	0.407
tr|Q7KTW5|Q7KTW5_DROME	Q7KTW5	CG9391	3	3	0		0	0	0		2	1		0	0		0.117	0.407
sp|O97477|INO1_DROME	O97477	Inos	3	3	0		3	0	0		2	1		1	1		0.597	0.613
sp|P13238|VTU2_DROME	P13238	Vm26Ab	0	5	0		0	0	0		2	2		0	0		0.374	0.407
sp|Q9VMP9|GNPI_DROME	Q9VMP9	Gnpda1	0	5	0		0	0	0		2	2		0	0		0.374	0.407
tr|O97121|O97121_DROME	O97121	Eip55E	0	5	0		0	0	0		2	2		0	0		0.374	0.407
tr|Q2MGK5|Q2MGK5_DROME	Q2MGK5	CG4970	0	5	0		0	0	0		2	2		0	0		0.374	0.407
tr|Q8SXR1|Q8SXR1_DROME	Q8SXR1	NLaz	0	5	0		0	0	0		2	2		0	0		0.374	0.407
tr|Q8SYA4|Q8SYA4_DROME	Q8SYA4	CG18107	0	5	0		0	0	2		2	2		1	1		0.590	0.609
sp|P04359|RL32_DROME	P04359	RpL32	5	0	0		0	0	0		2	2		0	0		0.374	0.407
sp|Q9VRJ9|OTU1_DROME	Q9VRJ9	CG4603	5	0	0		0	0	0		2	2		0	0		0.374	0.407
tr|E1JJG7|E1JJG7_DROME	E1JJG7	CG32770	5	0	0		0	0	0		2	2		0	0		0.374	0.407
tr|Q0E9E2|Q0E9E2_DROME	Q0E9E2	CG1516	5	0	0		0	0	0		2	2		0	0		0.374	0.407

tr|Q4TWT4|Q4TWT4_DROME	Q4TWT4	su(r)	5	0	0		0	0	0		2	2		0	0		0.374	0.407
tr|Q9VSL4|Q9VSL4_DROME	Q9VSL4	GstO2	5	0	0		0	0	0		2	2		0	0		0.374	0.407
tr|Q7KUQ2|Q7KUQ2_DROME	Q7KUQ2	CG9674-RB	4	1	0		0	0	0		2	1		0	0		0.197	0.407
tr|O97428|O97428_DROME	O97428	cib	2	3	0		2	4	0		2	1		2	1		0.879	0.883
sp|Q02645-1|HTS_DROME	Q02645	hts	1	4	0		0	0	0		2	1		0	0		0.267	0.407
sp|Q9VNT5|TRXR2_DROME	Q9VNT5	Trxr-2	4	0	0		0	0	0		1	1		0	0		0.374	0.407
tr|A1Z8U4|A1Z8U4_DROME	A1Z8U4	Cct5	4	0	0		0	0	0		1	1		0	0		0.374	0.407
tr|A8DYP0|A8DYP0_DROME	A8DYP0	Unc-89	4	0	0		0	0	0		1	1		0	0		0.374	0.407
tr|Q24062|Q24062_DROME	Q24062	b	4	0	0		0	0	0		1	1		0	0		0.374	0.407
tr|Q9VFF0|Q9VFF0_DROME	Q9VFF0	CG3731	4	0	0		0	0	0		1	1		0	0		0.374	0.407
tr|Q9VH01|Q9VH01_DROME	Q9VH01	Bruce	4	0	0		4	0	0		1	1		1	1		0.940	0.940
tr|Q7JVI6|Q7JVI6_DROME	Q7JVI6	GstE13	3	1	0		0	0	0		1	1		0	0		0.171	0.407
sp|Q95083|PSA5_DROME	Q95083	Prosalpha5	1	3	0		0	0	0		1	1		0	0		0.147	0.407
sp|Q9XZJ4|PSA6_DROME	Q9XZJ4	Prosalpha1	1	3	0		0	0	0		1	1		0	0		0.147	0.407
tr|Q967S0|Q967S0_DROME	Q967S0	Prat2	1	3	0		0	0	0		1	1		0	0		0.147	0.407
tr|Q7KSB5|Q7KSB5_DROME	Q7KSB5	CG4390	1	3	0		0	3	0		1	1		1	1		0.694	0.703
sp|Q6NN85-1|SSH_DROME	Q6NN85	ssh	0	4	0		0	0	0		1	1		0	0		0.374	0.407
sp|Q9V813|MTAP_DROME	Q9V813	CG4802	0	4	0		0	0	0		1	1		0	0		0.374	0.407
sp|Q9VXX8|RL371_DROME	Q9VXX8	RpL37a	0	0	4		0	0	0		1	1		0	0		0.374	0.407
tr|A1Z8G7|A1Z8G7_DROME	A1Z8G7	Listericin	0	4	0		0	0	0		1	1		0	0		0.374	0.407
tr|A8QI34|A8QI34_DROME	A8QI34	CG40625	0	4	0		0	0	0		1	1		0	0		0.374	0.407
tr|B7YZX6|B7YZX6_DROME	B7YZX6	CG10600	0	4	0		0	0	0		1	1		0	0		0.374	0.407
tr|B7Z076|B7Z076_DROME	B7Z076	CG6852	0	0	4		0	0	0		1	1		0	0		0.374	0.407
tr|O97479|O97479_DROME	O97479	Sodh-1	0	4	0		0	0	0		1	1		0	0		0.374	0.407
tr|Q8INQ3|Q8INQ3_DROME	Q8INQ3	CG11760-RB	0	4	0		0	0	0		1	1		0	0		0.374	0.407
tr|Q9U9B0|Q9U9B0_DROME	Q9U9B0	gig	0	0	4		0	0	0		1	1		0	0		0.374	0.407
tr|Q9VPI8|Q9VPI8_DROME	Q9VPI8	net	0	0	4		0	0	0		1	1		0	0		0.374	0.407
tr|Q9VWS5|Q9VWS5_DROME	Q9VWS5	CG15040	0	0	4		0	0	0		1	1		0	0		0.374	0.407
tr|Q9W137|Q9W137_DROME	Q9W137	CG4707	0	0	4		0	0	0		1	1		0	0		0.374	0.407
tr|Q0E8H9|Q0E8H9_DROME	Q0E8H9	Hexo1	0	4	0		0	3	0		1	1		1	1		0.795	0.802
sp|Q9NIV1|E2AK3_DROME	Q9NIV1	PEK	4	0	0		0	0	0		1	1		0	0		0.374	0.407
sp|Q9V3J1-1|VATH_DROME	Q9V3J1	VhaSFD	4	0	0		0	0	0		1	1		0	0		0.374	0.407
tr|Q9VIQ8|Q9VIQ8_DROME	Q9VIQ8	CoIV	4	0	0		0	0	0		1	1		0	0		0.374	0.407
tr|Q9VKM3|Q9VKM3_DROME	Q9VKM3	l(2)06225	4	0	0		0	0	0		1	1		0	0		0.374	0.407
tr|A1Z784|A1Z784_DROME	A1Z784	ACC	2	1	0		0	0	0		1	1		0	0		0.141	0.407
tr|Q0E993|Q0E993_DROME	Q0E993	Aats-val	2	1	0		0	0	0		1	1		0	0		0.141	0.407
tr|Q1RL06|Q1RL06_DROME	Q1RL06	GS	1	0	2		2	0	0		1	1		1	1		0.476	0.494